Engineered Antibody and Monobody Domains with T Cell Receptor-Like Selectivity for Tumor Associated Peptide-MHC Antigens

Thesis by
Samy Hamdouche

In Partial Fulfillment of the Requirements for the degree
of
Doctor of Philosophy

CALIFORNIA INSTITUTE OF TECHNOLOGY
Pasadena, California
2014
(Defended May 29, 2014)

ACKNOWLEDGEMENTS

I would like to thank my thesis advisor and mentor, Stephen Mayo, for welcoming me into his lab, first as an undergraduate summer student and then as a PhD student. I thank him not only for offering me the resources and insight to accomplish the research described in this thesis, but also for providing me the support and autonomy to pursue the research path to which I was drawn. He has been an inimitable influence on my development as a graduate student and on my future career.

I would also like to acknowledge my colleagues and lab mates, who educated and trained me through this critical period in my career. In particular, I thank Matthew Moore, Alex Nisthal, Toni Lee, Bernardo Araujo Sosa Padilla, Alexandria Berry, Tim Wannier, Emzo de los Santos, Kurt Mou, Seth Lieblich, Jan Kostecki, Jackson Cahn, Andrew Lim, Rhonda DiGiusto, Mary Ary, and Mohsen Chitsaz. A special debt of gratitude is owed to Gene Kym, who has been an extraordinary collaborator throughout my graduate education; I look forward to our continued progress and success in the future.

I further express my gratitude to other members of the Caltech community who contributed to my training and research, including Michael Bethune, Geoffrey Lovely, Rachel Galimidi, and Jost Vielmetter. Additionally, I acknowledge my thesis committee- Thomas Miller, Niles Pierce, and David Baltimore, for their enlightened input and for pushing me to strive for the highest standards. I thank Mark Davis for his valued mentorship and friendship. I also thank Weston Nichols, who has been an unmatched teammate for the last five years; I am exhilarated to see what the next five years will have in store for us.

Finally, I thank my family, and especially my mother, whose sacrifices and unquestioned support toward my lifelong educational journey have been extraordinary. I love you with all of my heart.

ABSTRACT

Monoclonal antibody (mAb)-based therapeutics have established themselves as meaningful components of the treatment paradigm for a variety of tumors. However, since the approval of rituximab in 1997 as the first mAb-based therapy for cancer, there has been a paucity of novel, validated cancer targets for therapeutic intervention by mAbs. In effect, numerous challenges lie in the discovery of suitable extracellular or transmembrane antigens that permit the differentiation of tumor from healthy tissue. The adaptive immune system, though, mediates recognition of foreign antigens derived from the intracellular proteome by T cell receptor (TCR) binding to peptide-loaded major histocompatibility complex (pMHC) molecules. Because cancer is associated with large-scale alterations in the genome, there are a vast number of novel epitopes presented to the adaptive immune system. Although natural TCRs have exquisite functionality in distinguishing these foreign epitopes, and several tumor-reactive TCRs have, in fact, been characterized, the molecules themselves are poorly developable as therapeutic candidates. Thus, in order to enable TCR-like binding of a broader class of protein agents, this study explores the transfer of TCR binding domains to other mAb-based scaffolds, including the fibronectin-derived Fn3 and the IgG-derived 4D5 scaffolds. By using a combination of rational design and directed evolution to guide binding domain transfer, evidence for TCR-like binding was demonstrated for several engineered molecules. In addition to conferring binding functionality, the grafted TCR domains had a deleterious effect on the biophysical properties of these inherently robust protein scaffolds. Thus, this work provides novel insight into the objective of developing mAb-based agents with TCR-like binding specificity for pMHC antigens, informing future efforts to target the abundance of intracellular tumor epitopes.

TABLE OF CONTENTS

LIST OF TABLES AND FIGURES

ABBREVIATIONS

ACT	adoptive cell therapy
ADCC	antibody-dependent cellular cytotoxicity
APC	antigen-presenting cell
BiTE	bispecific T cell engager
CAR	chimeric antigen receptor
CDC	complement-dependent cytotoxicity
CDR	complementarity-determining region
ER	endoplasmic reticulum
Fab	fragment of antigen binding
FACS	fluorescence activated cell sorting
Fc	constant fragment
FcRn	neonatal Fc receptor
Fn3	human 10^{th} type III fibronectin domain
HLA	human leukocyte antigen
K_d	equilibrium dissociation constant
mAb	monoclonal antibody
MHC	major histocompatibility complex
PBS	phosphate-buffered saline
PBSF	phosphate-buffered saline with 0.1% w/v bovine serum albumin
PCR	polymerase chain reaction
pMHC	peptide-major histocompatibility complex

scFv	single-chain variable fragment
SPR	surface plasmon resonance
TAA	tumor-associated antigen
TCR	T cell receptor
T_m	denaturation midpoint temperature of a protein
V_H	heavy chain variable fragment
V_L	light chain variable fragment

C h a p t e r 1

INTRODUCTION

Antibody-based therapeutics are effective for the treatment of various cancers

Since the advent of hybridoma technology in 1975, the development of novel monoclonal antibodies (mAbs) as therapeutics has been actively and fruitfully pursued [2]. Generally, mAbs possess two distinct functional units: the constant fragment (Fc) and the fragment of antigen binding (Fab). In IgGs, the most frequently used class of mAb for immunotherapy, the Fc region mediates immune effector functions, such as antibody-dependent cellular cytotoxicity (ADCC) and complement-dependent cytotoxicity (CDC), and modulates pharmacokinetics by binding to neonatal Fc receptor (FcRn). The Fab domain contains the variable region, comprising six hypervariable complementarity-determining regions (CDRs) that bind antigen and confer specificity.

Over the past two decades, mAbs have increasingly demonstrated effectiveness in the treatment of patients with cancer. Therapeutic mAbs specifically target antigens expressed on the tumor cell surface (Her2, EGFR, CD20) or proteins in the tumor microenvironment that promote malignant growth and immune evasion (VEGF, CTLA-4). These mAbs act through antagonizing the function of a pro-tumorigenic ligand or receptor, modulating the immune system through Fc-mediated effector function, or by delivering a specific drug or radioactive isotope to the tumor [3]. Furthermore, mAbs may require the concerted action of several of these functions to exert clinical efficacy [4]. In addition to IgG therapeutics, several protein drug candidates have emerged that make use of non-antibody molecular recognition scaffolds. Similar to mAbs, alternative non-antibody scaffolds exert a pharmacological effect by binding to a physiological target, and may also be coupled to an effector domain, such as an Fc or cytotoxin [5]. For the purposes of this work, alternative scaffolds are classified under the general category of mAb-based proteins.

A key challenge in the development of therapeutic mAbs for oncology has been to identify antigens that are suitable targets for therapeutic intervention. In order for an acceptable

therapeutic window to exist, a target must be differentially expressed, mutated, or sufficiently overexpressed in the tumor relative to healthy tissue; alternatively, the ablation of biological function of the target or of cells expressing the target must be tolerated (e.g. CD20, CD19) [6]. The challenges in identifying targets that fit these criteria are apparent in the scarcity of targets of therapeutic mAbs approved for cancer (Table 1-1). In particular, much of the focus in the development of cancer immunotherapies has been to optimize effector function (by modifying Fc interactions or conjugating to cytotoxins) or to improve the safety (by eliminating non-human sequences) of mAbs against extensively validated targets. Although such efforts have generated incremental improvements in the treatment of certain cancers, it will be essential to discover and validate novel targets in order to expand the types of tumors that can be treated with mAb-based therapies.

The adaptive immune system provides a means of identifying the molecular signatures of tumors

T cells regulate the process of immune surveillance, in which the adaptive immune system is capable of identifying and eliminating somatic cells expressing exogenous proteins. The ability of T cells to identify target cells is modulated by the recognition of major histocompatibility complex (MHC)-restricted antigens, presented on somatic and professional antigen-presenting cells (APCs), by the T cell receptor (TCR), a heterodimeric immunoglobulin superfamily member expressed on the surface of T cells. In somatic cells, MHC class I molecules assemble in the endoplasmic reticulum (ER) with peptides that are generated from the degradation of intracellular proteins by the proteasome [7]. In professional APCs, MHC class II molecules in late endosomal compartments associate with peptides generated from the degradation of extracellular proteins by lysosomal proteases [8].

One of the striking features of T cells is their exquisite specificity in distinguishing foreign antigens from self-peptides, as well as their sensitivity to a sparse distribution of foreign antigens among a large population of presented self-peptides [9]. The diversity of peptide-MHC (pMHC) antigens that TCRs are able to recognize is programmed by the clonal variability of their CDRs, generated by VJ and V(D)J recombination during T cell development in the thymus. Structurally, the CDRs determine recognition of MHC-restricted antigens through loop-mediated contacts; CDRs 1 and 2 on both subunits interact primarily with the MHC surface, and the CDR3 of both

subunits interact primarily with the exposed antigen epitope (Figure 1-1) [10]. For $CD8^+$ T cells recognizing MHC class I-restricted antigens on somatic cells, recognition initiates a signaling cascade within the T-cell that ultimately results in the destruction of the infected cell. For $CD4^+$ T cells recognizing MHC class II-restricted antigens on professional APCs, recognition initiates the release of cytokines that enhances the clearance of pathogens by both humoral and cell-mediated mechanisms [11].

The theory of cancer immunoediting has emerged over the past several decades to explain the role of the adaptive immune system in the pathology of cancer. In particular, tumors may express proteins that are differentially upregulated, contain oncogenic mutations, have atypical post-translational modifications, or are normally expressed only in germline cells (and are thus novel to the adult immune system) [12]. Differential presentation by tumors of epitopes from these proteins is sometimes sufficient to activate a clonal population of T cells that can recognize these tumor-associated antigens (TAAs), resulting in an immune response. The first observation of T cell mediated antitumor immunity was in mice that, when pre-immunized with a syngeneic tumor, rejected subsequent tumor challenges [13]. In addition, the rejection of transplanted tumors was observed in mice that were not pre-immunized, but were transferred lymphocytes from pre-immunized mice [14].

The development of novel *in vitro* detection and cloning methods that can probe patient-derived T cells isolated from the infiltrate of autologous tumors led to the identification of human TCRs specific for MHC-restricted tumor antigens, including the Mart1 melanoma differentiation antigen and the Ny-Eso-1 cancer-testis antigen [15]. Several TCRs specific for MHC-restricted TAAs have since been identified, creating a repertoire of molecules that can target the intracellular tumor proteome [16].

Efforts at targeting MHC-restricted TAAs signal promise

Initial efforts at targeting MHC-restricted TAAs have focused on the utilization of tumor-specific T cells. A landmark study by Rosenberg and colleagues in 1988 demonstrated that the adoptive transfer of *ex vivo*-expanded tumor-infiltrating lymphocytes extracted from resected melanomas resulted in the specific lysis of autologous tumor cells in humans with metastatic melanoma [17].

The use of adoptive cell therapy (ACT) for the treatment of metastatic melanoma has since been extensively validated; objective responses have been observed in up to fifty percent of patients refractory to all other treatments options, with several reported complete responses [18].

More recent studies have demonstrated that normal human lymphocytes can be genetically engineered to recognize cancer antigens and mediate cancer regression *in vivo* [19]. After the successful cloning of the genes encoding TCRs specific for various cancer antigens, normal human lymphocytes could be transduced with a retrovirus encoding the TCRs [15]. The TCR-engineered lymphocytes may then be transferred to patients with metastatic melanoma, illustrating that ACT can be applicable to patients who do not possess a sufficient quantity of tumor-reactive cells to be expanded *ex vivo*.

Despite the promise of ACT, the utility of this method for the treatment of melanoma and other tumors has been limited. Indeed, challenges related to the scalability of the ACT process and the heterogeneity inherent to cell-based therapies have impeded regulatory and commercial success [20]. Furthermore, TCR gene-modified T cells for ACT express both the transduced TCR and the endogenous TCR; since TCRs are heterodimers, the concurrent expression of both dimers may lead to mispaired TCRs [21]. Such mispairing may then result in reduced functionality of the T cells, or unknown specificities that may result in off-target toxicities. An ACT approach that bypasses the issue of endogenous TCR chain mispairing is chimeric antigen receptor (CAR) T-cell therapy, in which the T cell is engineered to express an antibody single-chain Fv (scFv) domain fused to the intracellular signaling domains of the CD3-ζ chain and the costimulatory molecule 4-1BB [22]. Specifically, the recognition of the B cell antigen CD19 by the expressed scFv initiates a signaling cascade that results in the elimination of healthy and malignant B cells. Because the entire protein fusion containing the recognition and signaling domain is encoded by a single polypeptide chain, there is no concern of mispairing. In order to generalize the CAR technique to enable targeting of MHC-restricted antigens, it would be essential to create a single-chain construct capable of specifically recognizing pMHC. Consequently, attempts engineer single-chain analogs of the TCR V-domains have been pursued, with limited success due to the inherent instability of V-domain dimers in the absence of constant domains [23].

In order to circumvent the concerns intrinsic to cell therapies, there is an incentive to engineer pMHC-targeted therapies without the need for cellular components. Bent Jakobsen and

colleagues have developed a class of protein reagents, ImmTACs, to bind to pMHC TAAs and elicit an effector response by recruiting T cells to the pMHC-expressing tumor [24]. Specifically, ImmTACs comprise two domains- a stabilized TCR molecule and an anti-CD3 scFv- fused together by a flexible linker. The stabilized TCR domain is engineered for improved affinity and stability by introducing a non-native interchain disulfide bond in the constant region, and by extensively mutagenizing the CDR and framework regions of the TCR extracellular domain [25]. These steps are especially significant as TCRs are generally unstable and not well soluble in their native format, and have relatively low affinity for cognate pMHC [26]. Alternatively, the anti-CD3 scFv serves to localize and activate T cells in a polyclonal manner, similar to the approach employed by the bispecific T cell engager (BiTE) mAbs [27]. Notably, the potency of the anti-CD3 effector function may be critical given the low copy number (as low as 10 to 150 copies per cell) of any given pMHC target relative to targets of established mAb therapeutics [28].

Despite the recent success of ImmTACs, there are several potential drawbacks to the platform. For instance, not all TCRs may convert well to ImmTAC format, due to either the incompatibility of certain frameworks with the engineered interchain disulfide bond or the lack of expression of certain constructs in display format [29]. Furthermore, the introduction of copious non-native mutations increases the probability of eliciting and immunogenic response *in vivo* [30]. The use of degenerate codon libraries, while increasing the combinatorial diversity of sequences, may increase the likelihood of cross-reactivity to non-target pMHC by creating binders to novel epitopes or by biasing the interaction toward the conserved MHC helices [31]. Indeed, a structural study of a thus engineered, high affinity variant of the 2C TCR revealed that the gain of affinity was the direct consequence of tighter binding to the MHC residues [32].

Monoclonal antibody-based approaches to pMHC recognition

In order to avert the concerns related to employing TCR-based scaffolds, several groups have focused on the engineering of mAbs against pMHC by exploiting classical techniques. Efforts to raise mAbs by immunization and hybridoma technologies have used peptide-pulsed cells [33], soluble pMHC [34], and soluble pMHC tetramer [35] as immunogens. The latter approach, developed by Weidanz and colleagues has been especially effective in isolating mAbs against several different pMHC targets [36]. Concurrently, various groups have used phage display

technology in order to isolate pMHC-slective mAbs from immunized murine [37], pre-immune [38], or synthetic [39] phage libraries.

A major drawback associated with using classical antibody engineering techniques to target pMHC antigens is the difficulty of achieving peptide specificity. Because the peptide epitope comprises a small fraction of the exposed surface of a pMHC, such techniques may yield high affinity interactions between the mAb and pMHC antigen that do not necessarily include contacts at the MHC-peptide interface. These interactions are undesired because they would lead to cross-reactivity with MHC displaying irrelevant peptide antigen. Indeed, it is not possible with current methods to limit the selection of antibodies to clones that bind the desired peptide epitope; such clones must be identified post-selection by further analysis of selected binders, which increases the downstream cost and risk of failure.

Particularly, in cases where interactions between engineered mAbs and pMHC have been elucidated, the results are quite provocative. An analysis of determined co-crystal structures between TCRs and pMHC reveals that these interfaces possess a large buried surface area of interaction with the peptide epitope and a high degree of shape complementarity with exposed peptide residues [40]. Furthermore, the structures affirm a conserved binding mode in which the TCR is oriented diagonally relative to the long axis of the MHC peptide-binding groove, with the Vα domain located over the N-terminal portion of the peptide and the Vβ domain positioned above the C-terminal segment of the peptide. Likely, the forces of evolution and the process of selection in the thymus drive the TCR-pMHC interactions toward a binding mode that is optimized for specificity and sensitivity. In contrast, an X-ray crystal structure of the interaction between the engineered Fab Hyb3 and its target, HLA-A1-MAGE-A1, demonstrates considerable deviation form a normal TCR-like binding footprint [41]. Specifically, binding is shifted toward the C-terminal portion of the peptide, suggesting a more promiscuous binding mode in which alternative peptides ligands may conceivably be accommodated. Indeed, T cells constructed with Hyb3 fused to the TCR signaling domain lacked peptide specificity and killed HLA-A1-positive cells irrespective of peptide presentation [42].

Thus, it appears critical that the interaction between a pMHC and a protein binder be suitably positioned to be optimal for affinity and specificity. Because nature has provided a template, in the embodiment of TCRs, for such an optimized binding mode, it would seem desirable to emulate

TCR-like binding in the discovery of mAb-based agents targeting pMHC. Although there are drawbacks to using TCRs themselves as targeting agents, it would be reasonable to apply the concept of binding domain transfer in order to confer the binding elements of TCRs to suitable alternative protein scaffolds.

Binding domain transfer enables mimicry of TCR binding mode

Binding domain transfer is the method of grafting key residues from a binding molecule onto a different molecular recognition scaffold. This technique involves the identification of hotspots (amino acid residues critical to a specific binding interaction) or a contiguous sequence of residues that govern binding (e.g. a CDR loop), followed by the transplantation of the residues to suitable positions on the target scaffold, and often accompanied by the diversification of surrounding positions on the target scaffold to accommodate the new mutations [43]. Several examples of successful transplantation of single loops have been reported, including the grafting of CDR-H3 from an integrin binding antibody to an exposed loop of tissue-type plasminogen activator [44], grafting of CDR3 from a camelid VHH targeting lysozyme to the bacterial chromoprotein neocarzinostatin [45], and grafting of CDR-H1 from a CD4 binding antibody to the protein inhibitor of neuronal nitric oxide synthase [46]. The transfer of smaller binding elements between proteins has also been demonstrated successfully. For instance, the RGD hotspot from fibronectin that modulates binding to integrins was grafted onto an exposed loop of the cysteine-knot protein AgRP; flanking residues were then randomized with degenerate codons, and functional, integrin-binding clones were selected using yeast display [47]. In another example, three noncontiguous hotspot residues from erythropoietin were grafted onto suitable positions of the unrelated protein PLCδ_1-PH; computational design was used to generated explicit sequence variants that were screened for binding to the erythropoietin receptor *in vitro* [48]. The simultaneously grafting of multiple loops has also been established, a notable example of which is the technique of mAb humanization, whereby multiple CDR loops from non-human mAbs are transferred onto appropriate human antibody frameworks in order to reduce the immunogenicity of therapeutic mAbs [49].

The selection of an appropriate target scaffold is a critical step in the process of domain transfer. Indeed, several criteria are used to assess the fitness of a target scaffold for the grafted binding

elements, including sequence and structural homology [50] and three dimensional orientation and positioning of proposed grafting loci [51]. In most cases, the transfer of binding elements must be accompanied by diversification of surrounding residues of the target scaffold to recover loss of stability or affinity resulting from the chimerism. Techniques used to introduce sequence diversity include random mutagenesis and computational design. The latter option has typically been employed in cases where the target scaffold is rich in secondary structure, so that the conformation of the mutant scaffold may be reliably predicted [52]. In the cases where the binding elements comprise loop regions, methods such as site-directed mutagenesis and error-prone polymerase chain reaction (PCR) are preferred [53].

A consequence of using random mutagenesis for the diversification of target scaffolds is the requirement of relatively large libraries for generating sufficient diversity to identify functional clones. Consequently, ultra high-throughput techniques for screening or selection of positive binding, including phage and yeast display, are often necessary. In phage display, a library of approximately 10^{10} protein variants, encoded by a plasmid incorporating a genetic fusion to a bacteriophage coat protein, is transformed into a phage-competent bacterial host. The bacteria then produce phage mutants displaying library variants that can be panned against immobilized target, enabling the isolation of positive binding clones for reinfection and outgrowth of subsequent bacterial culture [54]. By contrast, yeast display entails the genetic fusion of scaffold mutants to the Aga2p mating adhesion receptor on the surface of *S. cerevisiae* [55]. Fluorescently labeled target protein can then be used to stain yeast, from which cells displaying positive binding clones are selected using fluorescence activated cell sorting (FACS). Whereas phage display is often preferred for naïve or synthetic libraries because of the capacity for screening a larger number of variants (yeast libraries are typically 10^8 in size), yeast display is often preferred when using affinity maturation techniques, such as error-prone PCR, as yeast homologous recombination circumvents several cloning steps. Furthermore, eukaryotic hosts lessen the expression biases characteristic of bacterially propagated libraries [55].

The presence of binding hotspots in the CDR loops of TCRs has been demonstrated using alanine scanning mutagenesis, in which alanine substitution mutants are assayed for binding to the usual binding partner [56]. In particular, the binding affinity of the alanine mutant relative to that of the wild-type protein is used to compute a difference in free energy of binding between the two variants, which reveals the relative contribution of a residue's side chain to a binding interaction.

Alanine scanning experiments of TCR-pMHC interfaces reveal that several TCRs contain residues that contribute disproportionately to binding of pMHC (Table 1-2). Such studies provide a rationale for grafting these key residues, contained in CDR loops, onto a suitable target scaffold in order to replicate the archetypal TCR binding mode. As a result, the affinity and specificity of a TCR may be transplanted onto a more appropriate framework for developing protein therapeutics.

Fn3 and 4D5 are suitable target scaffolds for TCR binding domain transfer

The evaluation of target scaffolds for TCR domain transfer should depend on several criteria. Chiefly, a suitable scaffold must have ideal characteristics to be developable as a mAb-based therapeutic- including high stability, capacity to be engineered (i.e. in a display format), and low immunogenicity. Ideally, such a scaffold would also have close structural homology to the TCR framework in order to correctly position and orient the grafted hotspots and thus maximize the likelihood of successful domain transfer. Because TCRs possess the very prevalent immunoglobulin-like fold, characterized by beta-sandwich domains containing flexible loops flanked by alternating beta strands, homology exists with several proteins in the immunoglobulin superfamily [57].

Among the structural homologues of TCRs, the most relevant is perhaps the Fab fragment of antibodies. In fact, before the first TCR structure was elucidated, sequence analyses correctly predicted that TCRs would have a domain topology and binding orientation similar to those of Fabs [58]. Among the Fab frameworks, perhaps the most established for therapeutic use is 4D5, a human scaffold corresponding to the germ-line sequences IGVH 3–66 and IGVK 1–39 (IMGT nomenclature). In addition to constituting the framework of the therapeutic mAb Herceptin, 4D5 has demonstrated a robust capacity to be engineered, as it is the basis for several reported antibody libraries and has been engineered to bind several different antigens by diversification of its CDR loops [59-61]. 4D5 furthermore exhibits high heterologous expression yields and above average thermodynamic stability [62]. Notably, CDR grafting to 4D5 has previously been used to rescue the poor thermodynamic stability and soluble expression yield of a murine anti-fluorescein antibody, providing further rationale for transfer of TCR loops [63].

In addition to 4D5, the Fn3 scaffold, based on the human 10th type III fibronectin domain, is also a candidate for TCR binding domain transfer. Fn3 is a 10 kDa single-chain beta-sandwich with seven beta-strands and three loops clustered on each pole, and has comparable structure and geometry to the TCR Vα domain (Figure 1-2). In addition, Fn3 has a high thermodynamic stability, and has been used as an alternative non-antibody scaffold (known as "monobody") to engineer binders against several targets in various display formats to affinities as high as 1 pM [64]. Notably, an Fn3-based drug candidate targeting vascular endothelial growth factor receptor 2 is currently being evaluated in clinical trials for oncology indications, with preliminary evidence of repeated dose safety and anti-tumor activity [65].

Chapter 2 of this thesis examines the binding domain transfer from known tumor-specific TCRs to Fn3. In particular, yeast display libraries are constructed by grafting onto the loops of Fn3 the corresponding CDR loops from the Vα domain of TCRs specific for human leukocyte antigen (HLA) A2 in complex with a peptide derived from the melanoma differentiation antigen Mart1. The target HLA-A2-Mart1 is chosen because it is an established MHC-restricted TAA for which several well-characterized TCRs are known to bind [66]. Specifically, the determined co-crystal structures for the complex between the TCRs and HLA-A2-Mart1 may enable structural modeling and examination of selected Fn3 sequences, in order to determine whether key residues governing the interaction are conserved following mutagenesis.

Similarly, Chapter 3 of this thesis investigates the binding domain transfer from known tumor-specific TCRs to 4D5. Relative to Fn3, 4D5 is a less stable scaffold; namely, the thermodynamic stabilities of 4D5 and Fn3 determined by similar methods are 8.1 kcal/mol and 12.6 kcal/mol, respectively [67, 68]. Although the lower stability of 4D5 may negatively impact its evolvability in general [69], it has significantly closer sequence and structural homology to the TCR framework, and may thus be a better candidate for TCR chimeragenesis. Furthermore, the demonstration of successful domain transfer onto an additional scaffold would serve to illustrate the efficacy of the general technique of TCR binding domain transfer. In addition to investigating the binding domain transfer of HLA-A2-Mart1-specific TCRs, Chapter 3 examines the transfer of CDR loops from a TCR specific for HLA-A2 in complex with a peptide derived from the cancer-testis antigen Ny-Eso-1[70]. The corresponding TCR, 1G4, is similarly well characterized with a determined co-crystal structure [71].

To construct diversified libraries of TCR-Fn3 and TCR-4D5 chimeras, a unique application of molecular cloning is exploited. In particular, to avoid loss of TCR-like pMHC selectivity, diversified positions must be carefully chosen so that potential hotspot residues from parental TCRs are preserved. However, because the precise hotspots residues for the Mart1- and Ny-Eso-1-specific TCRs are not known, the implementation of traditional site-directed mutagenesis with degenerate nucleotides libraries is problematic. Instead, error-prone PCR is preferred as a method of diversification, as it can be tuned to introduce combinatorial mutations across long gene segments more conservatively than degenerate nucleotides [72]. The specific cloning method, a variation of a protocol used to create synthetic Fn3 libraries [73], is adapted to accommodate TCR-to-Fn3 binding domain transfer, and is further extended to TCR-to-4D5 binding domain transfer.

Target	Approved Therapy	Indication	Notes
Her2/Neu	Herceptin	Breast cancer	
	Kadcyla	Breast cancer	DM1-conjugated
	Perjeta	Breast cancer	
CD20	Rituxan	Lymphoma	Murine variable region
	Zevalin	Lymphoma	Radiolabeled (yttrium-90 or indium-111)
	Bexxar	Lymphoma	Radiolabeled (iodine-131)
	Gazyva	Lymphoma	Glyco-engineered Fc
	Arzerra	Lymphoma	Fully-human mAb
EGFR	Erbitux	Colorectal, head and neck	Chimeric IgG1
	Vectibix	Colorectal	Fully human IgG2
VEGF	Avastin	Colorectal	
CTLA-4	Yervoy	Melanoma	
CD30	Adcetris	Lymphoma	MMAE-conjugated

Table 1-1. FDA approved monoclonal antibody-based therapeutics for the treatment of cancer.

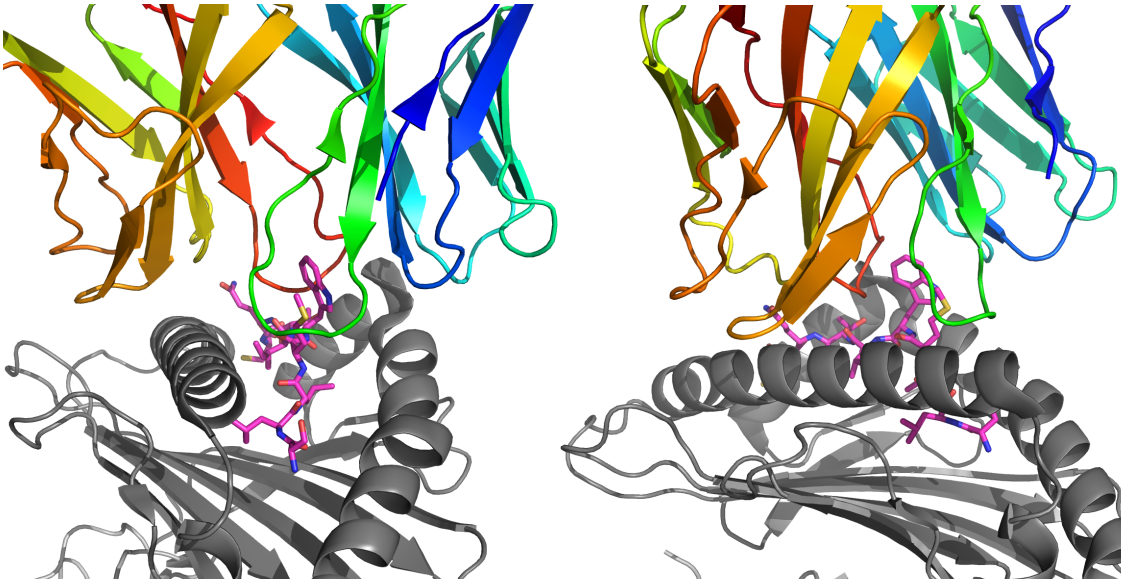

Figure 1-1. X-ray crystal structure of the ternary complex between a T cell receptor (rainbow), MHC class I molecule (gray), and an antigenic peptide (magenta). The CDR1α (blue) and CDR1β (yellow) interact primarily with MHC helices, while CDR3α (green) and CDR3β (red) predominantly contact peptide residues. PDB 2bnr.

T cell receptor	Antigen	PDB	Amino Acid	Position	Chain	ΔΔG (kcal/mol)
TCR LC13	B-8 EBV	1mi5	D	30A	Vα	1.64
TCR LC13	B-8 EBV	1mi5	H	33	Vα	1.64
TCR LC13	B-8 EBV	1mi5	H	48	Vα	1.12
TCR LC13	B-8 EBV	1mi5	L	50	Vα	1.64
TCR LC13	B-8 EBV	1mi5	P	93	Vα	1.64
TCR LC13	B-8 EBV	1mi5	L	94	Vα	1.64
TCR LC13	B-8 EBV	1mi5	Y	100	Vα	1.64
TCR LC13	B-8 EBV	1mi5	K	103	Vα	1.64
TCR LC13	B-8 EBV	1mi5	S	31	Vβ	1.06
TCR LC13	B-8 EBV	1mi5	Q	98	Vβ	1.64
TCR LC13	B-8 EBV	1mi5	Y	100	Vβ	1.64
TCR LC13	B-8 EBV	1mi5	Q	106	Vβ	1.64
TCR 2C	L(d)-QL9	2oi9	T	29	Vα	2.05
TCR 2C	L(d)-QL9	2oi9	Y	31	Vα	1.33
TCR 2C	L(d)-QL9	2oi9	Y	49	Vα	1.48
TCR 2C	L(d)-QL9	2oi9	Y	50	Vα	1.48
TCR 2C	L(d)-QL9	2oi9	L	104	Vα	1.42
TCR 2C	L(d)-QL9	2oi9	N	31	Vβ	1.48
TCR 2C	L(d)-QL9	2oi9	Y	48	Vβ	1.48
TCR 2C	L(d)-QL9	2oi9	Y	50	Vβ	1.48
TCR 1934	I-A(u) MBP	2pxy	Y	29	Vα	1.2
TCR 1934	I-A(u) MBP	2pxy	R	48	Vα	1.2
TCR 1934	I-A(u) MBP	2pxy	S	50	Vα	1.2
TCR 1934	I-A(u) MBP	2pxy	R	51	Vα	1.2
TCR 1934	I-A(u) MBP	2pxy	N	31	Vβ	1.2
TCR 1934	I-A(u) MBP	2pxy	Y	48	Vβ	1.2
TCR 1934	I-A(u) MBP	2pxy	Y	50	Vβ	1.2
TCR 1934	I-A(u) MBP	2pxy	E	56	Vβ	1.2
TCR 172	I-A(u) MBP	1u3h	L	50	Vα	2
TCR 172	I-A(u) MBP	1u3h	V	52	Vα	2
TCR 172	I-A(u) MBP	1u3h	N	31	Vβ	2
TCR 172	I-A(u) MBP	1u3h	Y	48	Vβ	2
TCR 172	I-A(u) MBP	1u3h	Y	50	Vβ	2
TCR 172	I-A(u) MBP	1u3h	E	56	Vβ	2
TCR JM22	A-2 Flu	1oga	S	32	Vα	1
TCR JM22	A-2 Flu	1oga	Q	34	Vα	1
TCR JM22	A-2 Flu	1oga	D	32	Vβ	1.6
TCR JM22	A-2 Flu	1oga	Q	52	Vβ	2
TCR JM22	A-2 Flu	1oga	I	53	Vβ	2
TCR JM22	A-2 Flu	1oga	N	55	Vβ	1.1
TCR JM22	A-2 Flu	1oga	R	98	Vβ	2

Table 1-2. Hotspot residues found in TCR-pMHC interfaces, where the definition of hotspot is taken to be a residue that, when mutated to alanine, results in a difference in free energy of binding (ΔΔG) of at least 1 kcal/mol. Data is compiled from the Alanine Scanning Energetics database (ASEdb) [1]. ΔG of binding is typically determined by SPR.

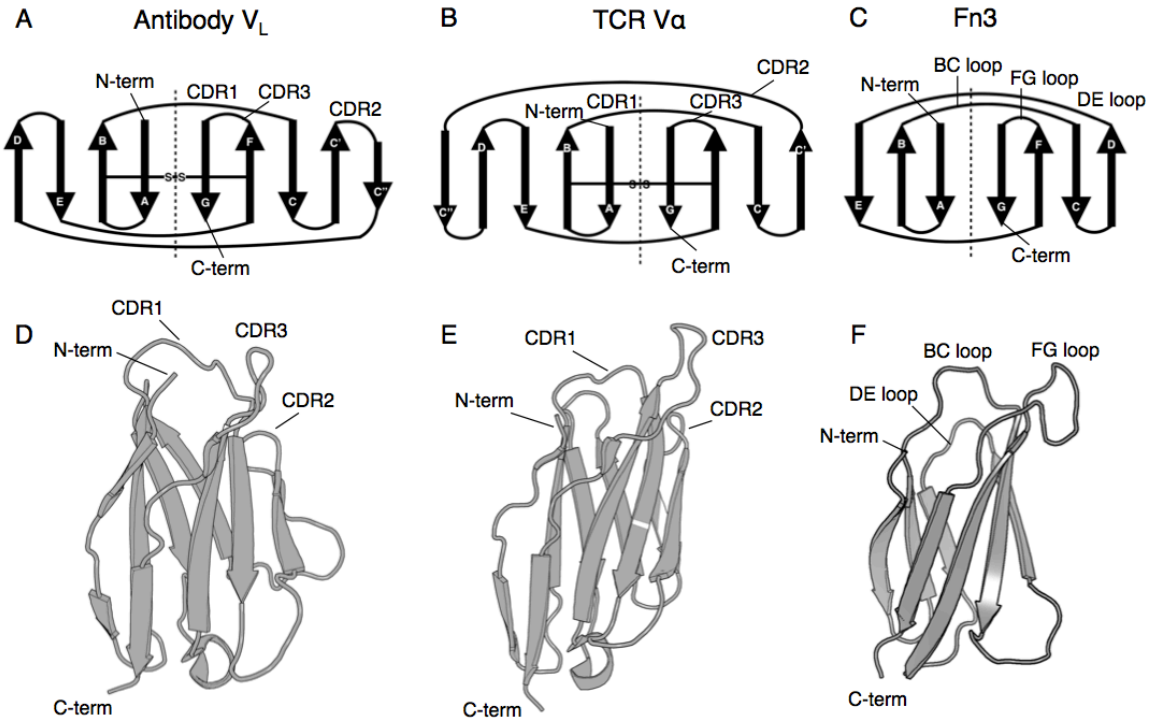

Figure 1-2. Topology diagrams comparing (A) the antibody light chain immunoglobulin fold, (B) the T cell receptor alpha chain immunoglobulin fold, and (C) the Fn3 immunoglobulin fold. Structures of (D) the antibody light chain domain of 4D5, (E) a TCR alpha chain domain, and (F) the Fn3, corresponding to PDB ID's 1n8z, 3qdg, and 1fna, respectively. Primary binding loops, as well as N- and C-termini are indicated.

References

1. Thorn, K.S. and A.A. Bogan, *ASEdb: a database of alanine mutations and their effects on the free energy of binding in protein interactions.* Bioinformatics, 2001. **17**(3): p. 284–5.

2. Kohler, G. and C. Milstein, *Continuous cultures of fused cells secreting antibody of predefined specificity.* Nature, 1975. **256**(5517): p. 495–7.

3. Hughes, B., *Antibody–drug conjugates for cancer: poised to deliver?* Nat Rev Drug Discov, 2010. **9**(9): p. 665–667.

4. Nimmerjahn, F. and J.V. Ravetch, *Antibodies, Fc receptors and cancer.* Current Opinion in Immunology, 2007. **19**(2): p. 239–245.

5. Weidle, U.H., et al., *The emerging role of new protein scaffold-based agents for treatment of cancer.* Cancer Genomics Proteomics, 2013. **10**(4): p. 155–68.

6. Nelson, A.L., E. Dhimolea, and J.M. Reichert, *Development trends for human monoclonal antibody therapeutics.* Nat Rev Drug Discov, 2010. **9**(10): p. 767–774.

7. Pamer, E. and P. Cresswell, *Mechanisms of MHC class I--restricted antigen processing.* Annu Rev Immunol, 1998. **16**: p. 323–58.

8. Jensen, P.E., *Recent advances in antigen processing and presentation.* Nat Immunol, 2007. **8**(10): p. 1041–8.

9. Huppa, J.B. and M.M. Davis, *T-cell-antigen recognition and the immunological synapse.* Nat Rev Immunol, 2003. **3**(12): p. 973–83.

10. Garboczi, D.N., et al., *Structure of the complex between human T-cell receptor, viral peptide and HLA-A2.* Nature, 1996. **384**(6605): p. 134–41.

11. Krogsgaard, M. and M.M. Davis, *How T cells 'see' antigen.* Nat Immunol, 2005. **6**(3): p. 239–45.

12. Robbins, P.F. and Y. Kawakami, *Human tumor antigens recognized by T cells.* Curr Opin Immunol, 1996. **8**(5): p. 628–36.

13. Old, L.J. and E.A. Boyse, *Immunology of Experimental Tumors.* Annual Review of Medicine, 1964. **15**(1): p. 167–186.

14. Hellstrom, K.E. and I. Hellstrom, *Cellular immunity against tumor antigens.* Adv Cancer Res, 1969. **12**: p. 167–223.

15. Hughes, M.S., et al., *Transfer of a TCR gene derived from a patient with a marked antitumor response conveys highly active T-cell effector functions.* Hum Gene Ther, 2005. **16**(4): p. 457–72.

16. Aleksic, M., et al., *Different affinity windows for virus and cancer-specific T-cell receptors: implications for therapeutic strategies.* Eur J Immunol, 2012. **42**(12): p. 3174–9.

17. Rosenberg, S.A., et al., *Use of tumor-infiltrating lymphocytes and interleukin-2 in the immunotherapy of patients with metastatic melanoma. A preliminary report.* N Engl J Med, 1988. **319**(25): p. 1676–80.

18. Dudley, M.E., et al., *Adoptive cell transfer therapy following non-myeloablative but lymphodepleting chemotherapy for the treatment of patients with refractory metastatic melanoma.* J Clin Oncol, 2005. **23**(10): p. 2346–57.

19. Morgan, R.A., et al., *Cancer regression in patients after transfer of genetically engineered lymphocytes.* Science, 2006. **314**(5796): p. 126–9.

20. Kalos, M. and Carl H. June, *Adoptive T Cell Transfer for Cancer Immunotherapy in the Era of Synthetic Biology.* Immunity, 2013. **39**(1): p. 49–60.

21. Reuss, S., et al., *TCR-engineered T cells: a model of inducible TCR expression to dissect the interrelationship between two TCRs.* (1521-4141 (Electronic)).

22. Kalos, M., et al., *T Cells with Chimeric Antigen Receptors Have Potent Antitumor Effects and Can Establish Memory in Patients with Advanced Leukemia.* Science Translational Medicine, 2011. **3**(95): p. 95ra73.

23. Aggen, D.H., et al., *Single-chain ValphaVbeta T-cell receptors function without mispairing with endogenous TCR chains.* Gene Ther, 2012. **19**(4): p. 365–74.

24. Liddy, N., et al., *Monoclonal TCR-redirected tumor cell killing.* Nat Med, 2012. **18**(6): p. 980–7.

25. Li, Y., et al., *Directed evolution of human T-cell receptors with picomolar affinities by phage display.* Nat Biotech, 2005. **23**(3): p. 349–354.

26. Shusta, E.V., et al., *Directed evolution of a stable scaffold for T-cell receptor engineering.* Nat Biotechnol, 2000. **18**(7): p. 754–9.

27. Bargou, R., et al., *Tumor regression in cancer patients by very low doses of a T cell-engaging antibody.* Science, 2008. **321**(5891): p. 974–7.

28. Purbhoo, M.A., et al., *Quantifying and imaging NY-ESO-1/LAGE-1-derived epitopes on tumor cells using high affinity T cell receptors.* J Immunol, 2006. **176**(12): p. 7308–16.

29. Boulter, J.M., et al., *Stable, soluble T-cell receptor molecules for crystallization and therapeutics.* Protein Engineering, 2003. **16**(9): p. 707–711.

30. Schellekens, H. and W. Jiskoot, *Immunogenicity of Therapeutic Proteins*, in *Pharmaceutical Biotechnology*, D.J.A. Crommelin, R.D. Sindelar, and B. Meibohm, Editors. 2013, Springer New York. p. 133–141.

31. Holler, P.D., L.K. Chlewicki, and D.M. Kranz, *TCRs with high affinity for foreign pMHC show self-reactivity.* Nat Immunol, 2003. **4**(1): p. 55–62.

32. Colf, L.A., et al., *How a Single T Cell Receptor Recognizes Both Self and Foreign MHC.* Cell, 2007. **129**(1): p. 135–146.

33. Porgador, A., et al., *Localization, quantitation, and in situ detection of specific peptide-MHC class I complexes using a monoclonal antibody.* Immunity, 1997. **6**(6): p. 715–26.

34. Polakova, K., et al., *Antibodies directed against the MHC-I molecule H-2Dd complexed with an antigenic peptide: similarities to a T cell receptor with the same specificity.* J Immunol, 2000. **165**(10): p. 5703–12.

35. Verma, B., et al., *Direct discovery and validation of a peptide/MHC epitope expressed in primary human breast cancer cells using a TCRm monoclonal antibody with profound antitumor properties.* Cancer Immunol Immunother, 2010. **59**(4): p. 563–73.

36. Weidanz, J.A., et al., *TCR-like biomolecules target peptide/MHC Class I complexes on the surface of infected and cancerous cells.* Int Rev Immunol, 2011. **30**(5-6): p. 328–40.

37. Andersen, P.S., et al., *A recombinant antibody with the antigen-specific, major histocompatibility complex-restricted specificity of T cells.* Proc Natl Acad Sci U S A, 1996. **93**(5): p. 1820–4.

38. Chames, P., et al., *Direct selection of a human antibody fragment directed against the tumor T-cell epitope HLA-A1-MAGE-A1 from a nonimmunized phage-Fab library.* Proc Natl Acad Sci U S A, 2000. **97**(14): p. 7969–74.

39. Miller, K.R., et al., *T cell receptor-like recognition of tumor in vivo by synthetic antibody fragment.* PLoS One, 2012. **7**(8): p. e43746.

40. Rudolph, M.G., R.L. Stanfield, and I.A. Wilson, *How TCRs bind MHCs, peptides, and coreceptors.* Annu Rev Immunol, 2006. **24**: p. 419–66.

41. Hülsmeyer, M., et al., *A Major Histocompatibility Complex·Peptide-restricted Antibody and T Cell Receptor Molecules Recognize Their Target by Distinct Binding Modes: CRYSTAL STRUCTURE OF HUMAN LEUKOCYTE ANTIGEN (HLA)-A1·MAGE-A1 IN COMPLEX WITH FAB-HYB3.* Journal of Biological Chemistry, 2005. **280**(4): p. 2972–2980.

42. Willemsen, R.A., et al., *T Cell Retargeting with MHC Class I-Restricted Antibodies: The CD28 Costimulatory Domain Enhances Antigen-Specific Cytotoxicity and Cytokine Production.* The Journal of Immunology, 2005. **174**(12): p. 7853–7858.

43. Kiss, C., et al., *Antibody binding loop insertions as diversity elements.* Nucleic Acids Res, 2006. **34**(19): p. e132.

44. Smith, J.W., K. Tachias, and E.L. Madison, *Protein loop grafting to construct a variant of tissue-type plasminogen activator that binds platelet integrin alpha IIb beta 3.* J Biol Chem, 1995. **270**(51): p. 30486–90.

45. Nicaise, M., et al., *Affinity transfer by CDR grafting on a nonimmunoglobulin scaffold.* Protein Sci, 2004. **13**(7): p. 1882–91.

46. Bes, C., et al., *PIN-bodies: a new class of antibody-like proteins with CD4 specificity derived from the protein inhibitor of neuronal nitric oxide synthase.* Biochem Biophys Res Commun, 2006. **343**(1): p. 334–44.

47. Silverman, A.P., et al., *Engineered Cystine-Knot Peptides that Bind αvβ3 Integrin with Antibody-Like Affinities.* Journal of Molecular Biology, 2009. **385**(4): p. 1064–1075.

48. Liu, S., et al., *Nonnatural protein–protein interaction-pair design by key residues grafting.* Proceedings of the National Academy of Sciences, 2007. **104**(13): p. 5330–5335.

49. Almagro, J.C. and J. Fransson, *Humanization of antibodies.* Front Biosci, 2008. **13**: p. 1619–33.

50. Lo, B.C., *Antibody Humanization by CDR Grafting*, in *Antibody Engineering*, B.C. Lo, Editor. 2004, Humana Press. p. 135–159.

51. Mandell, D.J. and T. Kortemme, *Computer-aided design of functional protein interactions.* Nat Chem Biol, 2009. **5**(11): p. 797–807.

52. Der, B.S. and B. Kuhlman, *From Computational Design to a Protein That Binds.* Science, 2011. **332**(6031): p. 801–802.

53. Binz, H.K., P. Amstutz, and A. Pluckthun, *Engineering novel binding proteins from nonimmunoglobulin domains.* Nat Biotechnol, 2005. **23**(10): p. 1257–68.

54. Winter, G., et al., *Making antibodies by phage display technology.* Annu Rev Immunol, 1994. **12**: p. 433–55.

55. Boder, E.T. and K.D. Wittrup, *Yeast surface display for screening combinatorial polypeptide libraries.* Nat Biotechnol, 1997. **15**(6): p. 553–7.

56. Manning, T.C., et al., *Alanine Scanning Mutagenesis of an αβ T Cell Receptor: Mapping the Energy of Antigen Recognition.* Immunity, 1998. **8**(4): p. 413–425.

57. Barclay, A.N., *Membrane proteins with immunoglobulin-like domains—a master superfamily of interaction molecules.* Seminars in Immunology, 2003. **15**(4): p. 215–223.

58. Claverie, J.M., A. Prochnicka-Chalufour, and L. Bougueleret, *Implications of a Fab-like structure for the T-cell receptor.* Immunol Today, 1989. **10**(1): p. 10–4.

59. Eigenbrot, C., et al., *X-ray structures of fragments from binding and nonbinding versions of a humanized anti-CD18 antibody: structural indications of the key role of VH residues 59 to 65.* Proteins, 1994. **18**(1): p. 49–62.

60. Chen, Y., et al., *Selection and analysis of an optimized anti-VEGF antibody: crystal structure of an affinity-matured Fab in complex with antigen.* J Mol Biol, 1999. **293**(4): p. 865–81.

61. Sidhu, S.S., et al., *Phage-displayed antibody libraries of synthetic heavy chain complementarity determining regions.* J Mol Biol, 2004. **338**(2): p. 299–310.

62. Willuda, J., et al., *High thermal stability is essential for tumor targeting of antibody fragments: engineering of a humanized anti-epithelial glycoprotein-2 (epithelial cell adhesion molecule) single-chain Fv fragment.* Cancer Res, 1999. **59**(22): p. 5758–67.

63. Jung, S. and A. Pluckthun, *Improving in vivo folding and stability of a single-chain Fv antibody fragment by loop grafting.* Protein Eng, 1997. **10**(8): p. 959–66.

64. Bloom, L. and V. Calabro, *FN3: a new protein scaffold reaches the clinic.* Drug Discovery Today, 2009. **14**(19–20): p. 949–955.

65. Tolcher, A.W., et al., *Phase I and pharmacokinetic study of CT-322 (BMS-844203), a targeted Adnectin inhibitor of VEGFR-2 based on a domain of human fibronectin.* Clin Cancer Res, 2011. **17**(2): p. 363–71.

66. Borbulevych, O.Y., et al., *TCRs Used in Cancer Gene Therapy Cross-React with MART-1/Melan-A Tumor Antigens via Distinct Mechanisms.* The Journal of Immunology, 2011. **187**(5): p. 2453–2463.

67. Wörn, A. and A. Plückthun, *An intrinsically stable antibody scFv fragment can tolerate the loss of both disulfide bonds and fold correctly.* FEBS Letters, 1998. **427**(3): p. 357–361.

68. van der Walle, C.F., H. Altroff, and H.J. Mardon, *Novel mutant human fibronectin FIII9-10 domain pair with increased conformational stability and biological activity.* Protein Eng, 2002. **15**(12): p. 1021–4.

69. Bloom, J.D., et al., *Protein stability promotes evolvability.* Proc Natl Acad Sci U S A, 2006. **103**(15): p. 5869–74.

70. Gnjatic, S., et al., *NY-ESO-1: review of an immunogenic tumor antigen.* Adv Cancer Res, 2006. **95**: p. 1–30.

71. Chen, J.L., et al., *Structural and kinetic basis for heightened immunogenicity of T cell vaccines.* J Exp Med, 2005. **201**(8): p. 1243–55.

72. Cirino, P.C., K.M. Mayer, and D. Umeno, *Generating mutant libraries using error-prone PCR.* Methods Mol Biol, 2003. **231**: p. 3–9.

73. Hackel, B.J., A. Kapila, and K.D. Wittrup, *Picomolar affinity fibronectin domains engineered utilizing loop length diversity, recursive mutagenesis, and loop shuffling.* J Mol Biol, 2008. **381**(5): p. 1238–52.

Chapter 2

CONSTRUCTION AND SCREENING OF AN FN3-TCR LIBRARY ENABLES THE DISCOVERY OF AN HLA-A2-MART1-SELECTIVE CLONE

Abstract

The desirability of soluble, single-chain proteins that mimic the peptide-specific binding properties of T cell receptors (TCRs) has led to the identification of the human 10th type III fibronectin domain (Fn3) as a suitable scaffold for grafting of the TCR binding loops. In order to rationally transfer the binding domain of a Mart1-specific TCR to Fn3, a library assembly method was developed with the goal of maximal transfer of TCR residues involved in antigen binding and minimal perturbation of the Fn3 framework. A novel, mutagenized library assembly method was developed after initial screens in yeast display signaled that randomization of the library may be necessary to successfully transfer binding properties to the new scaffold. Subsequent screens and selections in yeast display led to the identification of an HLA-A2-Mart1 binding clone that was confirmed to be Mart1 selective. Expression and further characterization of the clone in soluble format demonstrated a reduction in yield and solubility relative to wild-type Fn3. However, binding to HLA-A2-Mart1 antigen was confirmed by surface plasmon resonance (SPR). Although the biophysical properties of the isolated clone are suboptimal, the results of the TCR-to-Fn3 binding domain transfer are quite instructive of future attempts to engineer molecules with TCR-like binding properties.

Introduction

In Chapter 1, the utility of a single-chain, soluble TCR-like binder to MHC-restricted tumor-associated antigens is established. Furthermore, a strong rationale is proposed for transferring the binding domains from TCRs onto homologous proteins, such as the antibody Fab and the Fn3 monobody domains. In this study, validation of the approach of TCR-to-Fn3 binding domain transfer is ventured by the engineering of a novel binder against HLA-A2-Mart1$_{26-35}$, a target of interest in oncology and, specifically, melanoma. Specifically, HLA-A2-Mart1 is targeted by the TCRs MEL5 [1], DMF4, and DMF5 [2], which have been well characterized biophysically.

Fn3 is a single chain, 10 kDa beta-sandwich with seven beta-strands and three loops arranged on each pole, and has comparable structure and geometry to the TCR Vα domain (Figure 1-2). In addition, Fn3 has a high thermodynamic stability, with a reported melting temperature (T_m) of 88°C, and has been used as a scaffold to engineer binders against several targets in various display formats with affinities as high as 1 pM [3]. Notably, an Fn3-based drug candidate targeting vascular endothelial growth factor receptor 2 is currently being evaluated in clinical trials for oncology indications, with preliminary evidence of repeated dose safety and anti-tumor activity [4].

Benjamin Hackel et al. [5] describe a method for Fn3 library assembly whereby amino acid sequence and length diversity can be introduced into the BC, DE, and FG loops. Following structural and topological comparison of the Fn3 and TCR Vα loops (Figure 2-1), the sequences of homologous loops from Mart1-specific TCRs may be targeted for replacement onto the Fn3 framework sequence. A library of Fn3 mutants containing loop grafts from these TCRs may be generated using an adaptation of the above polymerase chain reaction (PCR)-based assembly method. The techniques of yeast display and fluorescence activated cell sorting (FACS) may then enable the high-throughput screening and selection of positive binding clones.

Materials and Methods

Reagents and strains

The BirA-tagged and biotinylated extracellular domains of HLA-A2-Mart1 and HLA-A2-Ny-Eso-1 were provided by the NIH Tetramer Facility. Yeast display *Saccharomyces cerevisiae* strain EBY100, yeast display plasmid pPNL6, yeast secretion strain YVH10, and yeast secretion plasmid pPNL9 were obtained from Pacific Northwest National Laboratory. All yeast display protocols, buffers, and reagents were used as previously described [6, 7]. Oligonucleotides were obtained from Integrated DNA Technologies, and PCR assembly primers were designed using DNAWorks from NIH's Helix Systems [8]. Gene mutagenesis was performed by error-prone PCR as previously described [9], with nucleotide analogs from TriLink Biotechnologies. KOD Hot Start Polymerase from Novagen was used to PCR assemble gene inserts. The inserts have flanking 20-40 base pair overlaps with the desired cloning site in their respective, linearized plasmids. These were assembled into the appropriate plasmids using either yeast homologous recombination or Gibson cloning into TOP10 *Escherichia coli* cells. Reagents for Gibson cloning are as previously described [10], and constructs cloned into TOP10 competent cells were subsequently mini-prepped and transformed into yeast. Purification resins included HIS-select HF Nickel Affinity Gel from Sigma and StrepTactin Sepharose High Performance from GE Healthcare Life Sciences. Unless otherwise stated, all chemicals were from Sigma, and all *E. coli* strains from Life Technologies. Soluble protein expression was performed in 2.5 L Ultra Yield Flasks from Thomson. Protein was concentrated in Amicon 3,000 Da MWCO centrifugal filters from EMD Millipore. DNA extraction was performed with kits from Qiagen.

Loop grafts, error-prone mutagenesis, and library assembly

The Fn3 library was constructed to produce the wild-type sequence in the framework regions and to graft the CDR1α, CDR2α, and CDR3α sequences of HLA-A2-Mart1-specific TCRs onto the BC, DE, and FG loops of Fn3, respectively. In addition, loop grafts from structurally characterized non-Mart1-specific TCRs, were included, especially where the loops specifically contact the MHC helices, in order to increase the paratope diversity of the library. Excision points for the loop grafts were determined by structural alignment of Fn3 to the TCR Vα domains, comparing the distances between Cα atoms of residue pairs to appropriately demarcate the loops (Figure 2-1). Specifically, the DNA encoding for amino acids 23–31 (DAPAVTVRY) was

replaced by DNA encoding for the CDR1α residues 24-32; the DNA for amino acids 51–56 (PGSKST) was replaced by DNA encoding for the CDR2α residues 57-62; the DNA for amino acids 77–86 (GRGDSPASSK) was replaced by DNA encoding for the CDR3α residues 107-117. All residue numbers for TCRs correspond to the IMGT numbering designated for TRAV gene sequences. Double-stranded DNA corresponding to these loop fragments (with 30 base pairs of homology to adjoining framework regions), as well as double-stranded DNA corresponding to the constant framework regions, were prepared from pairs of complementary oligonucleotides by overlap extension PCR. The full-length Fn3 library was assembled as previously described [5], resulting in a small library (< 1000 unique clones) of Fn3-TCR chimeras.

Error-prone PCR directed solely at the solvent-exposed loops of this library was used to focus diversity on the likely paratope. Fn3 genes were constructed with conserved wild-type framework sequence and randomly mutated loops from the pool of Fn3-TCR chimeras assembled above. Error-prone PCR of the loop regions was performed via three separate 50 μL reactions with 20 mM 8-oxo-deoxyguanosine triphosphate and 20 mM 2'-deoxy-p-nucleoside-5'-triphosphate and primers flanking the BC, DE, and FG loops. The reaction mixtures were denatured at 94°C for 3 min, cycled 15 times at 94°C for 45s, 60°C for 30s, and 72°C for 90s, and finally extended at 72°C for 10 min. Multiple preliminary mutagenesis reactions of the wild-type plasmid were conducted at different nucleotide analog concentrations. Sequence analysis and comparison to a wild-type framework indicate that the aforementioned conditions produce one to five amino acid mutations per loop. The PCR products were purified by agarose gel electrophoresis and each amplified in four 100-μL PCR reactions containing 1× Taq buffer, 2 mM MgCl2, 1 μM of each primer, 0.2 mM (each) dNTPs, 4 μL of error-prone PCR product (of 40 μL from gel extraction), and 2.5 U of Taq DNA polymerase. The reactions were thermally cycled at the same conditions except that 35 cycles were used. The full-length Fn3 library was then assembled from the mutagenized loop fragments and constant framework fragments similarly to the non-mutagenized library above.

Yeast display, flow cytometry, and sorting

Yeast displayed protein was expressed at 20ºC and 250 RPM for 16 hours. Displayed protein was incubated with biotinylated monomeric HLA-A2-Mart1 or HLA-A2-Ny-Eso-1, or tetrameric peptide-MHC prepared by incubating streptavidin–fluorophore (R-phycoerythrin, AlexaFluor488;

Invitrogen, Carlsbad, CA) with biotinylated pMHC in a 1:4 ratio (four equal additions of fluorophore, 10 min in between additions, covered from light at room temperature) in phosphate-buffered saline (PBS). Flow cytometry was performed on a BD Biosciences FACSCalibur, and data was analyzed with FlowJo from Tree Star. 50,000 cell counts were collected for each binding analysis experiment. All yeast display experiments were performed in PBS with 0.1% w/v bovine serum albumin (PBSF) buffer as previously described [11]. Libraries were constructed by high efficiency yeast electroporation [7]. FACS was performed on the MoFlo XDP instrument from Beckman Coulter using polypropylene BD Falcon FACS tubes.

Measurement of K_d in yeast display

Affinity titrations to determine the equilibrium dissociation constant (K_d) for given clones were performed as previously described [12]. All incubations were performed while nutating at room temperature. Quenched samples were placed on ice in a 4ºC cold room. All work with cold samples was performed at 4ºC with chilled tips and a dedicated cold room centrifuge. Samples were handled in 1.5 mL Eppendorf tubes, and then transferred to a Nunc polypropylene 96-well V-bottom plate prior to addition of secondary reagents for ease of handling and standardization between samples. Prior to flow cytometry analysis, samples were spun down and kept as pellets on ice, covered from light. Immediately prior to analysis, individual samples were resuspended in 0.5 mL of PBSF and transferred to a polystyrene BD Falcon FACS tube for loading. 20,000 cell counts were collected for each sample in titration assays. Analysis was performed in GraphPad Prism version 6.0d for OSX 10.9 from GraphPad Software. K_d was fit to the Michaelis-Menten model.

Expression of soluble anti-Mart1 Fn3

Fn3 clones were expressed in YVH10 yeast secretion culture. YVH10 transformed with an Fn3 construct in pPNL9 with a 6×HIS tag were grown overnight in 6L of SDCAA–Ura. This was spun down and transferred to YPGR media (1% yeast extract, 2% bacto peptone, 2% galactose, 2% raffinose, 0.1% dextrose; denoted in w/v, yeast media components from BD Biosciences, sugars from Sigma) with penicillin-streptomycin from Life Technologies. This culture was expressed at 20ºC, 200 RPM, for 48 hours. Pellets were spun down and discarded twice, and the supernatant was ammonium sulfate (VWR) precipitated at 80% salt. Precipitate was resuspended in YVH10 binding/wash buffer (300 mM NaCl, 20 mM sodium phosphate, pH 7.8, 0.05% tween 20, 2.5% glycerol, 10 mM imidazole) and loaded onto HIS-select resin. After washing with the same buffer,

samples were eluted in YVH10 elution buffer (300 mM NaCl, 20 mM sodium phosphate, pH 7.8, 0.05% tween 20, 2.5% glycerol, 200 mM imidazole), concentrated, and run over an analytical Superdex-75 column from Amersham Pharmacia on the ÄKTA FPLC system. Sample volume was 0.5 mL, run at 0.5 mL/min in PBS. Typical yields were 0.1 mg/L from yeast secretion culture.

Characterization of soluble anti-Mart1 Fn3 by surface plasmon resonance

Surface plasmon resonance (SPR) experiments were performed as previously described [13] using a Biacore T200 instrument with CM5 sensor chips and HBS-EP$^+$ buffer (GE Healthcare) at 25°C. Streptavidin was first coupled to the sensor surface using amine coupling, and biotinylated HLA-A2-Mart1 was then immobilized at different densities to flow cells 2 through 4 of the streptavidin coated chip. Soluble anti-Mart1 Fn3 was flowed over the chip at twofold serial dilutions ranging from 1500 nM to 12 nM, with a buffer-only control to establish a baseline. Data were corrected for bulk solvent effects using a flow cell containing immobilized streptavidin only. Flow rates were 5 µl/min. Data were processed with Biacore T200 Evaluation Software (GE Healthcare).

Reversion clone construction

Reversion of engineered loops of anti-Mart1 Fn3 to the wild-type Fn3 sequence was achieved by PCR assembling the wild-type loop fragments with 30 base pairs of homology to the flanking framework regions, amplifying the plasmid backbone minus the targeted loop segment (round the horn PCR), and then assembling the backbone and fragment pairs by Gibson assembly [14]. Because the backbone is amplified from the anti-Mart1 Fn3 DNA contained in the pPNL6 backbone, assembly results in a complete gene within a yeast display vector.

Structural Modeling of anti-Mart1 Fn3

A structural model of the interaction between the anti-Mart1 Fn2 and HLA-A2-Mart1 was constructed using the AnchoredDesign package within the Rosetta 3.3 software suite [15]. This package was designed to model docked structures interacting through flexible surface loops where there is evidence for a particular binding mode. In this case, the FG loop of the Fn3 scaffold (PDB: 1fna) is aligned to the residues from the CDR3α of the DMF5 TCR that contact HLA-A2-Mart1 (PDB 3qdg) and are also contained in the anti-Mart1 Fn3. These residues are

called the anchor region, and form the basis for the hypothesized binding interaction between HLA-A2-Mart1 and the anti-Mart1 Fn3. Starting from this structure, and holding the anchor region constant, the FG loop of Fn3 is remodeled and minimized, and the side chains are repacked, as previously described [16]. The models were analyzed by calculating the Rosetta score, per-atom solvent accessible surface area, and shape complementarity, all using the Rosetta software package.

Results

Identification of a dominant clone

The error-prone library of Fn3 genes was incorporated into a yeast surface display system by homologous recombination with the pPNL6 vector incorporating an N-terminal Aga2 protein for display on the yeast surface and a C-terminal c-myc epitope for detection of full-length Fn3. Library transformation yielded 5×10^6 yeast transformants. A library size of 10^8 was expressed and subjected to five sequential fluorescence-activated cell sorting (FACS) sorts with decreasing concentrations of HLA-A2-Mart1 tetramer. Sorting against 200 nM for the first two sorts and 100 nM for the final three sorts, the top 1-5% of each population for both antigen binding and c-myc expression levels was collected for culture outgrowth (Figure 2-2). Each round was monitored by sequencing 10 clones at each step. By round five, the library converged upon a dominant clone with the sequence of PFTDSAIYGH in the BC loop, VTGSGS in the DE loop, and NFGGGKLIFGQ in the FG loop (Table 2-1).

Remarkably, the sequence of the FG loop contains no mutations relative to the CDR3α from TCR DMF5, suggesting strong selective pressure for the wild-type loop sequence. Structural analysis of this loop in the context of the DMF5 TCR (PDB 3qdg) demonstrates that the loop residues exclusively contact amino acids of the α2-helix of HLA-A2. A structural model determined by computationally grafting the selected loop sequences onto the Fn3 framework, preserving the contacts made between the DMF5 CDR3α with HLA-A2-Mart1, suggests that peptide selectivity is likely mediated by Tyr-30 of the engineered BC loop, which is positioned to contact Ile-5 of the Mart1 peptide (Figure 2-3). The engineered variant- anti-Mart1 Fn3- was selected for further experimental characterization and analysis.

Binding and selectivity of anti-Mart1 Fn3 in yeast display

Yeast displaying anti-Mart1 Fn3 were incubated with 100 nM HLA-A2-Mart1 tetramer or 100 nM HLA-A2-Ny-Eso-1 tetramer to determine the relative affinity of the clone to HLA-A2 presenting two different peptides. At this concentration of tetramer, anti-Mart1 Fn3 exhibits clear binding to HLA-A2-Mart1 and no detectable binding to irrelevant antigen (Figure 2-4). These data suggest that anti-Mart1 Fn3 is, in fact, selective for the Mart1 peptide.

An affinity titration was performed to determine the K_d at equilibrium. Yeast displaying anti-Mart1 Fn3 were incubated with varying concentrations of HLA-A2-Mart1 tetramer (0–2000 nM) for two hours. This experiment is not designed to determine the monovalent binding of anti-Mart1 Fn3 to HLA-A2-Mart1, because antigen is multivalently coupled to streptavidin-fluorophore (maximum valency of four). However, the binding affinity to tetramer was measured to be 927 ± 280 nM (Figure 2-5).

Characterization of soluble anti-Mart1 Fn3 by surface plasmon resonance

To confirm that anti-Mart1 Fn3 functions outside of display format, *S. cerevisiae* was used as a host to express and secrete the protein into the culture medium. Soluble anti-Mart1 Fn3 appears to be monomeric by comparison to FPLC standards (Figure 2-6). The purified protein was subsequently characterized for binding to HLA-A2-Mart1 monomer by surface plasmon resonance. Streptavidin was first coupled to the sensor chip, followed by injection and binding of biotinylated HLA-A2-Mart1 monomer (Figure 2-7). Varying concentrations of anti-Mart1 Fn3 were injected in order to obtain a binding isotherm and determine an equilibrium dissociation constant. However, such a determination was not possible because binding was not measured at sufficiently high concentrations of anti-Mart1 Fn3. Furthermore, whenever quantities of anti-Mart1 Fn3 were reduced in volume to a concentration exceeding the upper limit of this experiment, a visible precipitate materializes, and concentrations do not increase as measured by absorbance at 280 nm. This observation suggests that anti-Mart1 Fn3 is not well soluble in PBS. Nevertheless, the SPR data does demonstrate binding of soluble anti-Mart1 Fn3 to HLA-A2-Mart1, and that this binding exhibits a concentration dependence (Figure 2-7). Furthermore, the SPR trace qualitatively demonstrate that the binding kinetics exhibit a fast on-rate and fast off-rate, which are analogous to the kinetics of association and dissociation of the wild-type DMF5 TCR [2], suggesting a potentially similar mechanism of binding for the two molecules.

Reversion to wild-type loops

In an attempt to improve the solubility of anti-Mart1 Fn3 while retaining binding affinity and selectivity to HLA-A2-Mart1, the BC, DE, and FG loops were independently restored to their wild-type Fn3 sequence. Because Fn3 is known to be highly stable and well soluble in standard buffers [3], and because the loss of solubility in anti-Mart1 Fn3 is ostensibly due to the mutated and atypical length loops, the reversion of one or more loops to their original sequences may

recover the solubility properties characteristic of wild-type Fn3. However, when the reversion clones are assayed for binding to HLA-A2-Mart1 tetramer by yeast display, no detectable binding relative to anti-Mart1 Fn3 is observed (Figure 2-8). Thus, no further characterization of the reversion clones was pursued.

Discussion

In theory, Fn3 is an ideal scaffold target for TCR domain transfer across many criteria. For instance, it is extremely thermostable with a reported T_m of 88°C [17], monomeric, contains no cysteines, and is produced at high yields in *E. coli*. However, it is known that diversification of the BC, DE, and FG loops have a substantial deleterious effect on thermodynamic stability [5].

Although anti-Mart1 Fn3 is highly expressed in yeast display format, and binds selectively to HLA-A2-Mart1 in both yeast display and as a soluble protein, its utility as a molecular recognition agent is clearly encumbered by its poor solubility. As no other region of the protein differs from the wild-type Fn3 sequence, the loop regions are implicated in the poor solubility of anti-Mart1 Fn3. It may be possible that only a subset of residues in one or more loops contribute to its poor solubility; however, all loops appear to be required for binding, as reversion of any one loop to its wild-type sequence ablates binding affinity for HLA-A2-Mart1. The computed structural model suggests that MHC-restriction is mediated by the FG loop, while peptide selectivity is mediated by Tyr-30 of the BC loop (Figure 2-3). Notably, the DE loop is not predicted to make any contacts with antigen. However, during multi-loop diversification, selected sequences must provide not only proper intermolecular contacts for binding but also appropriate intramolecular contacts.

The apparent low affinity of anti-Mart1 Fn3 is expected, given that the assumed binding domain is derived from a TCR. In particular, the DMF5 TCR is reported to bind to HLA-A2-Mart1 with a K_d of 6 μM [2]. Because it is relatively straightforward, once a baseline of affinity has been established, to engineer a clone that expresses in yeast display format for greater affinity, the low affinity of anti-Mart1 Fn3 is not discouraging. For instance, multiple further rounds of directed evolution through focused or random mutagenesis could potentially increase affinity by several orders of magnitude [5]. Indeed, the computed structural model may inform efforts to mutagenize anti-Mart1 Fn3 in a site-directed manner, in order to increase its affinity for HLA-A2-Mart1 without sacrificing its peptide selectivity [18]. However, the persistence of poor solubility could be problematic, as a lack of selective pressure on the library for solubility could result in the continued selection of poorly soluble clones.

The low expression and solubility of anti-Mart1 Fn3 may be driven by either loss of thermodynamic stability following parallel grafting of TCR loop sequences, or by the presence of

aggregation-prone sequence elements. Indeed, because TCRs are physiologically expressed as transmembrane proteins, there is no selective pressure toward sequences amenable for soluble production. The loops grafted onto anti-Mart1 Fn3, though, are derived from TCRs that have been produced solubly in sufficient yields for crystallography, so the loop sequences may not themselves be susceptible to aggregation. In the context of a non-native Fn3 framework, however, the TCR sequences may impart a tendency to oligomerize. Additionally, although the solvent-exposed loop of Fn3 are more likely to tolerate sequence diversity than framework regions, the combination of multiple destabilizing alterations to Fn3 spawned from poorly stable TCRs may negatively impact the thermodynamic stability of the scaffold. In fact, solvent-exposed loops of several proteins have been determined to contain hotspots for both stabilizing and destabilizing mutations [19], and the imposition of non-native loop lengths onto the Fn3 framework may further promote destabilization. Because the relatively conservative error-prone PCR procedure employed in this study failed to recover adequate biophysical properties, it is clear that exceptional care must be given to promote stability and solubility of TCR-based chimeric libraries.

A potential solution to this challenge going forward could be to employ a method that would enable selection for protein solubility. One such method is the technique of secretion-and-capture yeast display, whereby the Fn3 library would be secreted by the host yeast strain before being anchored to the yeast cell wall by a strong, non-covalent interaction [20]. More specifically, the Fn3 library is genetically fused to a biotin acceptor peptide, to which heterologously co-expressed BirA enzyme site-selectively fuses a biotin moiety. Before library expression is induced, the surface of the yeast cells is covalently labeled with NHS-PEG-biotin and avidin. When the biotinylated Fn3 clones are secreted into the extracellular space, they strongly bind the surface-localized avidin, so that the clones are displayed on the surface of the yeast. Because the individual clones must be solubly secreted before they are surface-anchored, this method incorporates a selective pressure for the protein of interest to remain stable in solution. Thus, a potential advantage of this method is more efficient conversion from display to soluble production formats [20]. Combining this technique with a more comprehensive method of mutagenesis, including whole gene error-prone PCR [5], may increase the likelihood of selecting for soluble clones.

Another potential means of identifying clones that can be solubly produced may simply be to increase the hit rate of the library. Indeed, the size of the transformed library in this study (5×10^6) is rather small relative to typical yeast display campaigns reported [21], which may be orders of magnitude larger. Increasing the size of the library concurrently increases the number of binders present within the library, and selecting for these binders would yield multiple hits. These hits can subsequently be evaluated for solubility; the greater the number of hits that can be evaluated, the greater the likelihood of identifying a subset of clones that may be solubly produced.

A noteworthy consequence of this study is the discovery of an Fn3 clone comprising a wild-type CDR3α loop sequence in the FG loop. This loop, in the context of the DMF5 TCR, contributes to interactions with HLA-A2; the lack of mutations to the loop in anti-Mart1 Fn3 suggests that the FG loop adopts an analogous binding mode. In particular, the FG loop may anchor anti-Mart1 Fn3 to the α2-helix of HLA-A2 in a manner that positions the BC loop to contact the displayed peptide. It is intriguing to observe that the residues grafted from Vα domains can govern binding of anti-Mart1 Fn3 in the absence of any interactions mediated by Vβ. Importantly, though, the FG loop of anti-Mart1 Fn3 may provide a platform for future efforts to engineer Fn3-based binders to novel pMHC targets. In particular, by constructing libraries such that the FG loop is fixed to this specific sequence, and such that the BC and DE loops are diversified (i.e. with degenerate nucleotides), such libraries may bias interactions toward a binding mode that promotes peptide selectivity yet enables selection of clones that bind novel peptide antigens.

Conclusion

This study establishes that a Mart1-targeted library of diversified Fn3-TCR chimeras can yield a clone with measurable binding to HLA-A2-Mart1. These findings are notable in that they establish that the binding domains of TCRs, which typically express poorly in yeast display format [22], can be transferred to a homologous scaffold that displays efficiently. Furthermore, the resulting libraries are capable of producing clones that are peptide-selective. The latter finding is significant because a top hit from a naïve (synthetic or pre-immune) library would not *a priori* be expected to be peptide-selective, as there is no rationale for the selection of clones targeting the peptide epitope rather than any other molecular surface of the peptide-MHC molecule. However, the fact that the Fn3-TCR library was generated from TCRs known to make molecular contacts to peptides within the MHC groove biases the library toward peptide-selectivity. Because any top hits are already verified to display efficiently in yeast, they may form the basis for further diversification in order to engineer for greater affinity and, potentially, solubility (Figure 2-9). In contrast, the TCR clones from which the original Fn3-TCR library is derived are naturally recalcitrant to display formats and, accordingly, may not be amenable to further engineering.

Furthermore, the hypothesized role of the anti-Mart1 Fn3 FG loop in modulating binding to HLA-A2 enables the construction of Fn3 libraries, informed by structural models, that may yield selective binders against novel peptide epitopes. Thus, this work represents a promising approach to the generation of proteins with TCR-like selectivity for cognate peptide-MHC antigens. In order to increase the chances of success in future work exploiting this method, larger libraries may need to be generated (in order to increase the number of evaluable hits), and methods such as secretion and capture yeast display should be employed (in order to select for clones that transfer effectively from display to soluble format).

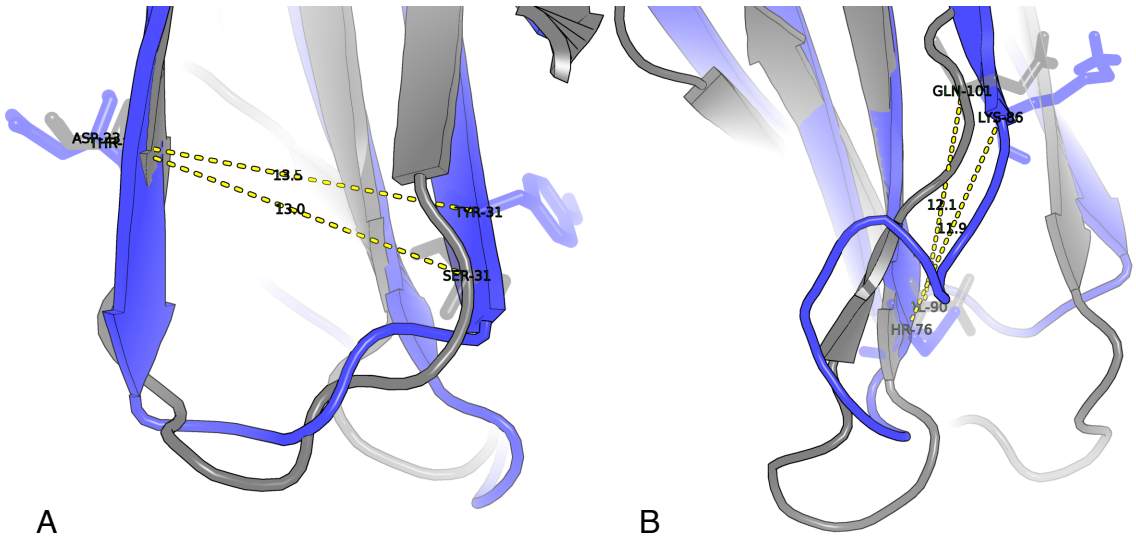

Figure 2-1. Structural alignment of Fn3 (gray) to the TCR Vα domain (blue). Recombination points for library generation are chosen at positions of homologous residue pairs on the BC loop and CDR1α (A), and on the FG loop and CDR3α (B). Structurally, distances between recombination endpoints on corresponding loops are roughly equivalent.

Loop	Sequence	Source TCR	WT TCR sequence	WT Fn3 sequence
BC	PFTDSAIYGH	TCR 1G4	SFTDSAIYNY	DAPAVTVRYY
DE	VTGSGS	TCR JM22	VTGGEG	PGSKST
FG	NFGGGKLIFGQ	TCR DMF5	NFGGGKLIFGQ	GRGDSPASSK

Table 2-1. Loop sequences of dominant clone anti-Mart1 Fn3. Amino acids that differ relative to the parental TCR sequence (resulting from error-prone PCR) are highlighted in red.

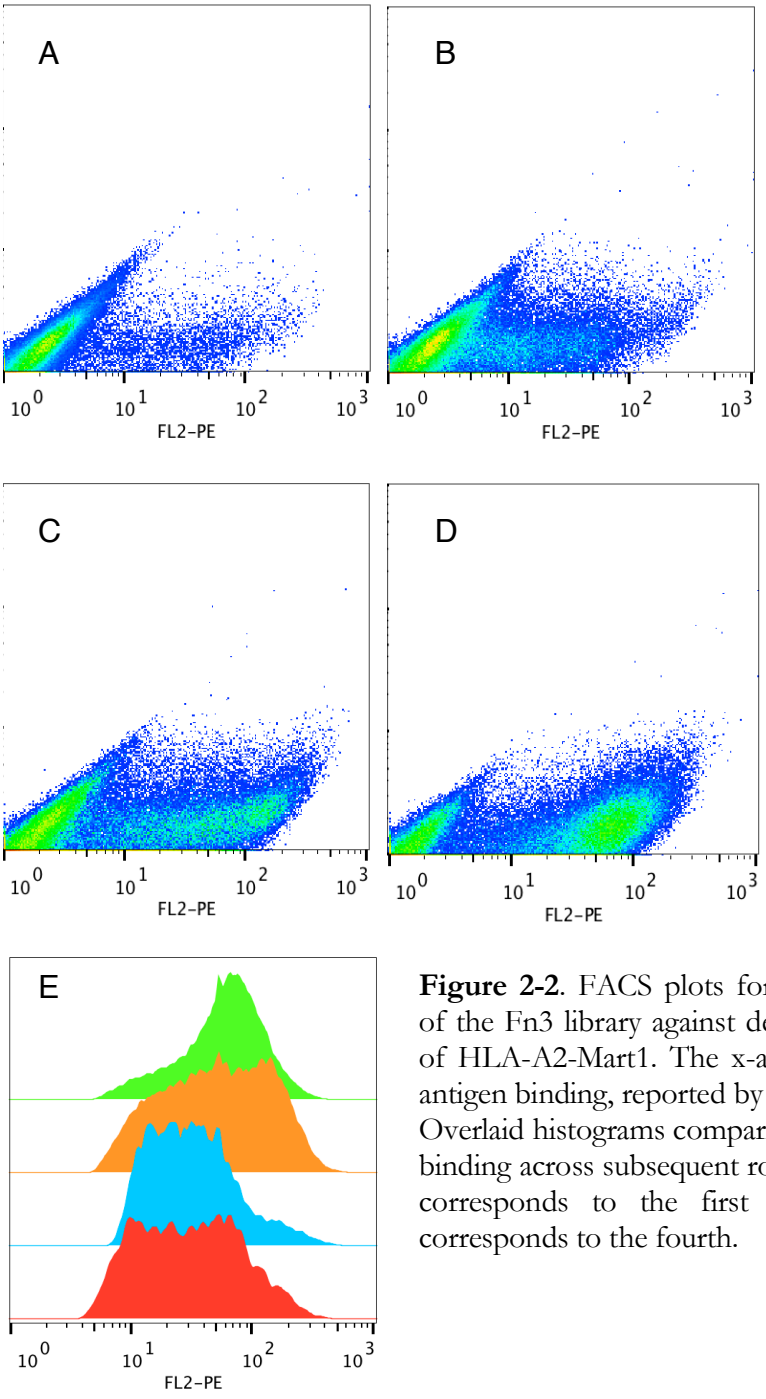

Figure 2-2. FACS plots for sequential sorts (A-D) of the Fn3 library against decreasing concentrations of HLA-A2-Mart1. The x-axes track the degree of antigen binding, reported by the fluorophore PE. (E) Overlaid histograms comparing the extent of antigen binding across subsequent rounds; the red histogram corresponds to the first round and the green corresponds to the fourth.

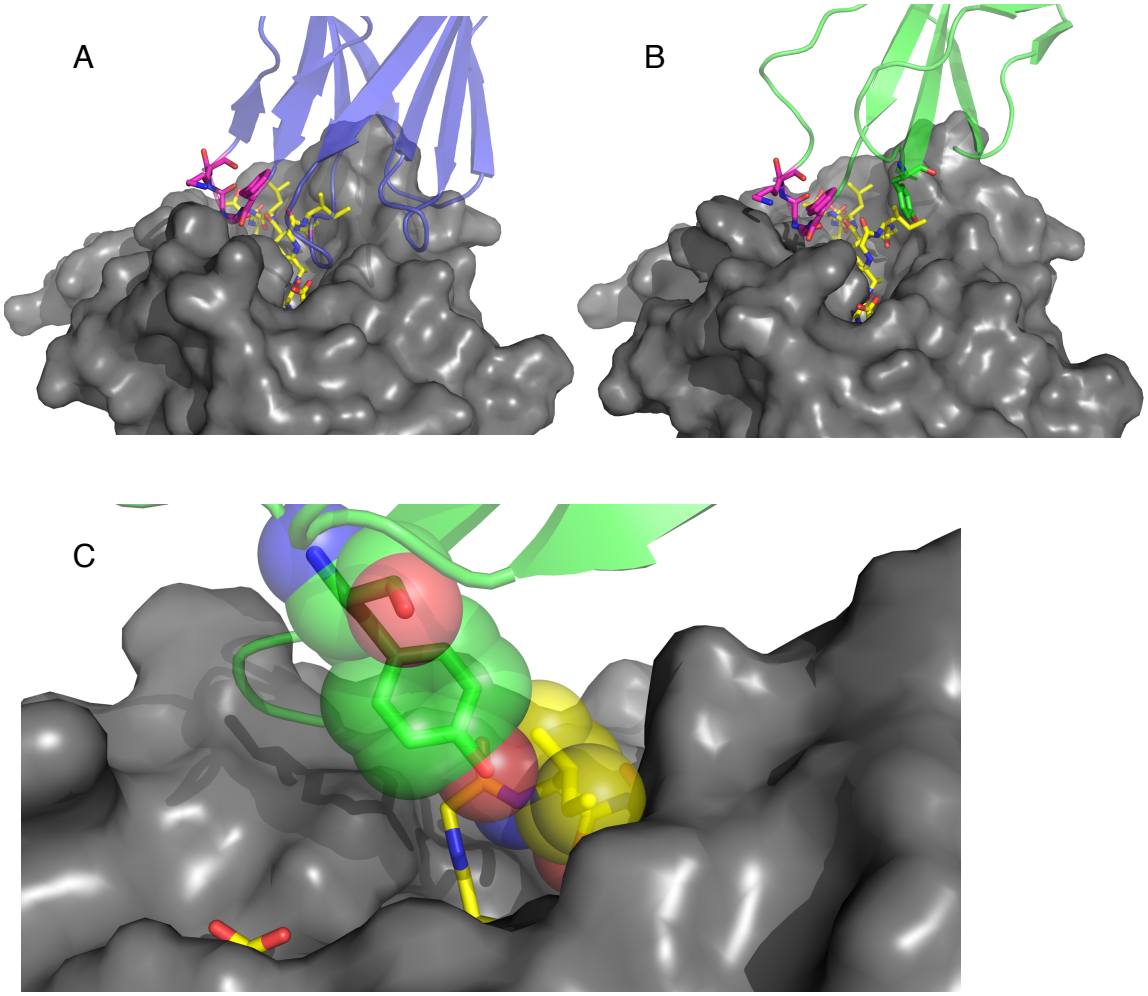

Figure 2-3. (A) Crystal structure of the DMF5 TCR alpha chain in complex with HLA-A2-Mart1. CDR3α (magenta) mediates interaction with the α2-helix of HLA-A2. (B) In the structural model of the interaction between anti-Mart1 Fn3 and HLA-A2-Mart1, the contacts mediated by the DMF5 CDR3α are assumed to be conserved, positioning Tyr-30 of the BC loop to contact Ile-5 of the Mart1 peptide (C).

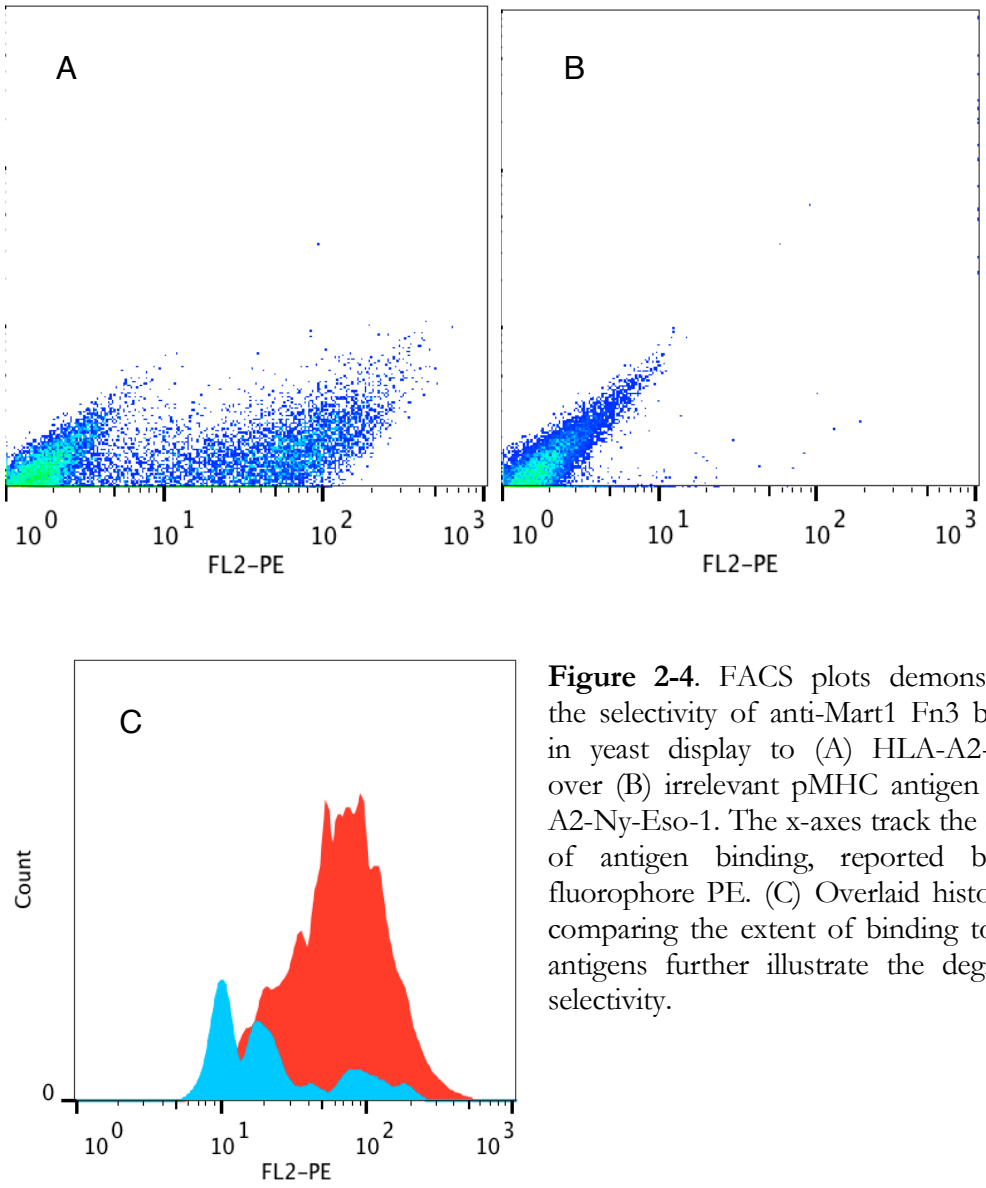

Figure 2-4. FACS plots demonstrating the selectivity of anti-Mart1 Fn3 binding in yeast display to (A) HLA-A2-Mart1 over (B) irrelevant pMHC antigen HLA-A2-Ny-Eso-1. The x-axes track the degree of antigen binding, reported by the fluorophore PE. (C) Overlaid histograms comparing the extent of binding to both antigens further illustrate the degree of selectivity.

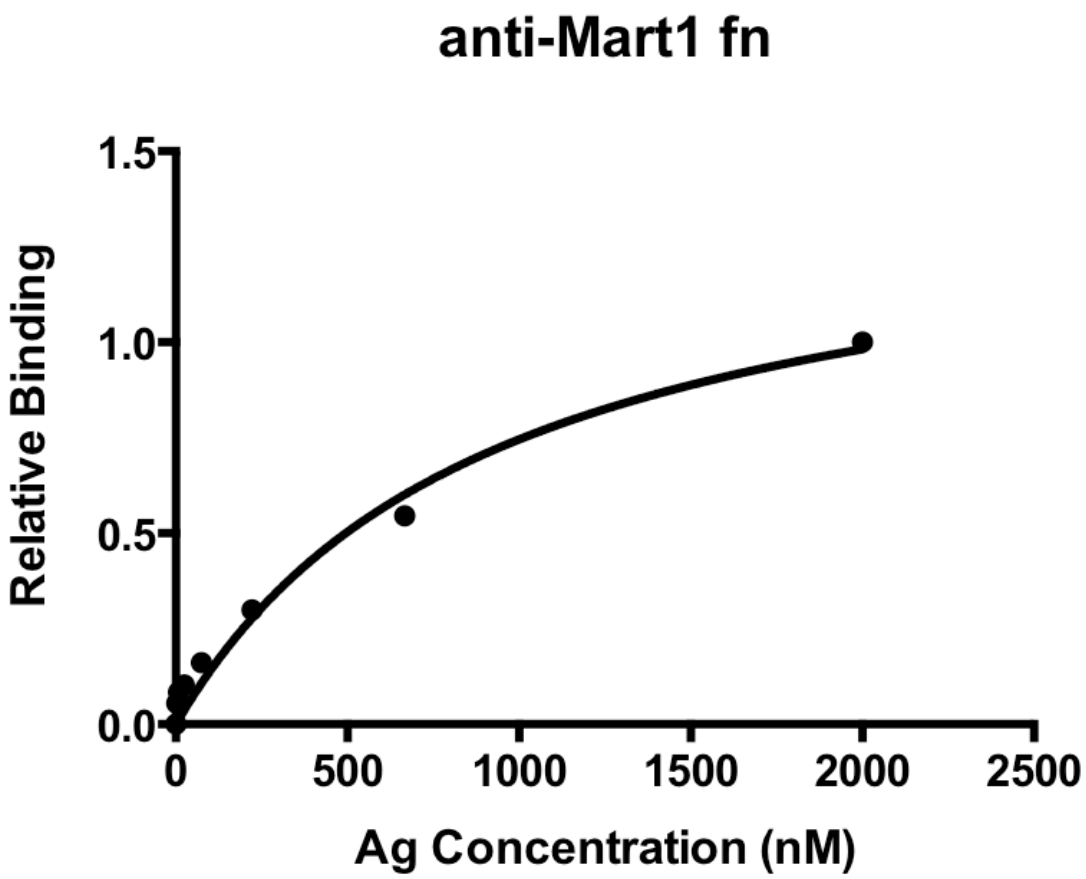

Figure 2-5. Equilibrium affinity titration of HLA-A2-Mart1 tetramer against displayed anti-Mart1 Fn3.

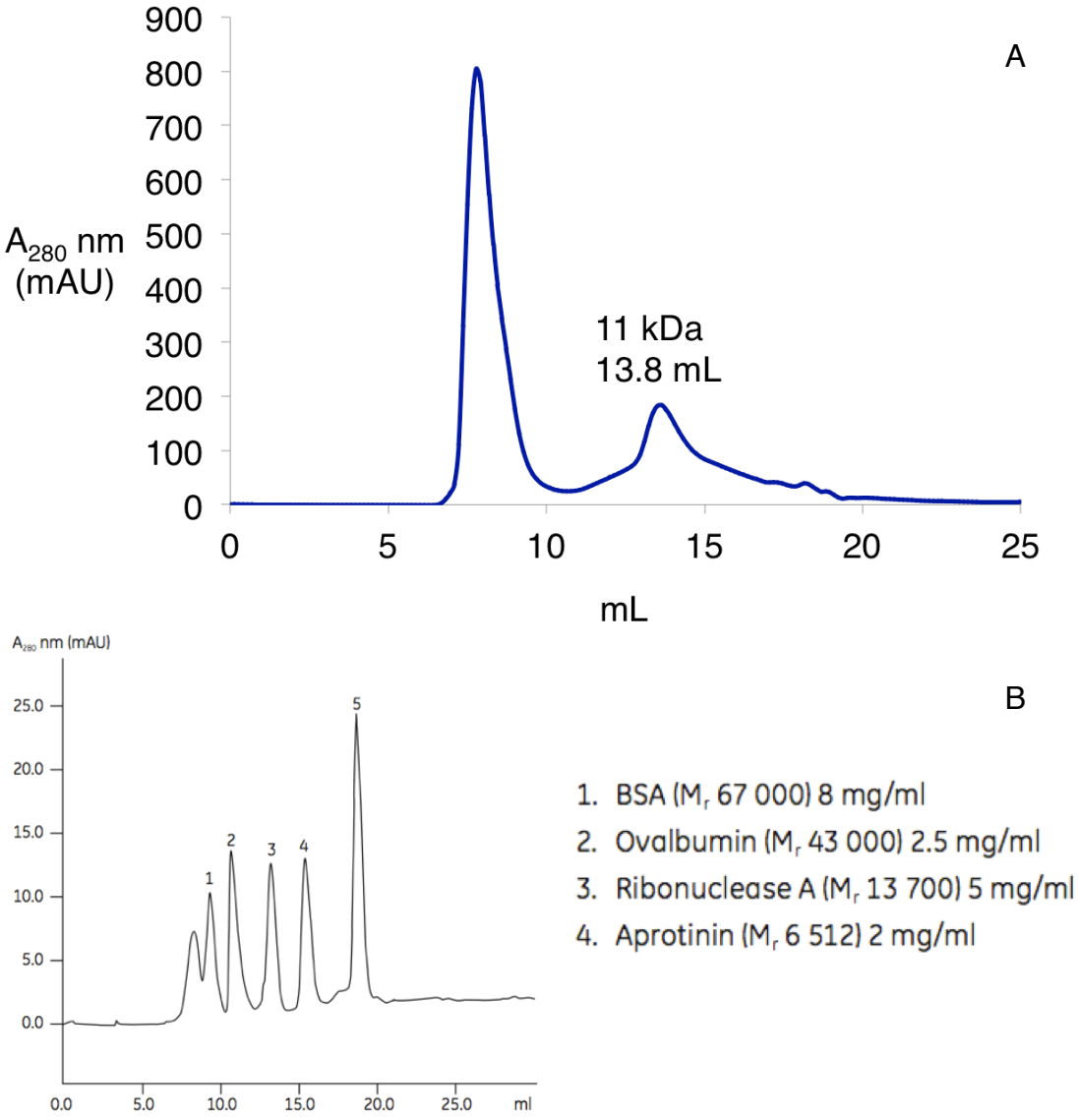

Figure 2-6. (A) Gel filtration profile of soluble anti-Mart1 Fn3. The major peak indicates the presence of soluble aggregate, while the minor peak corresponds to the expected monomeric profile. (B) Standards from the AKTA manual for comparison.

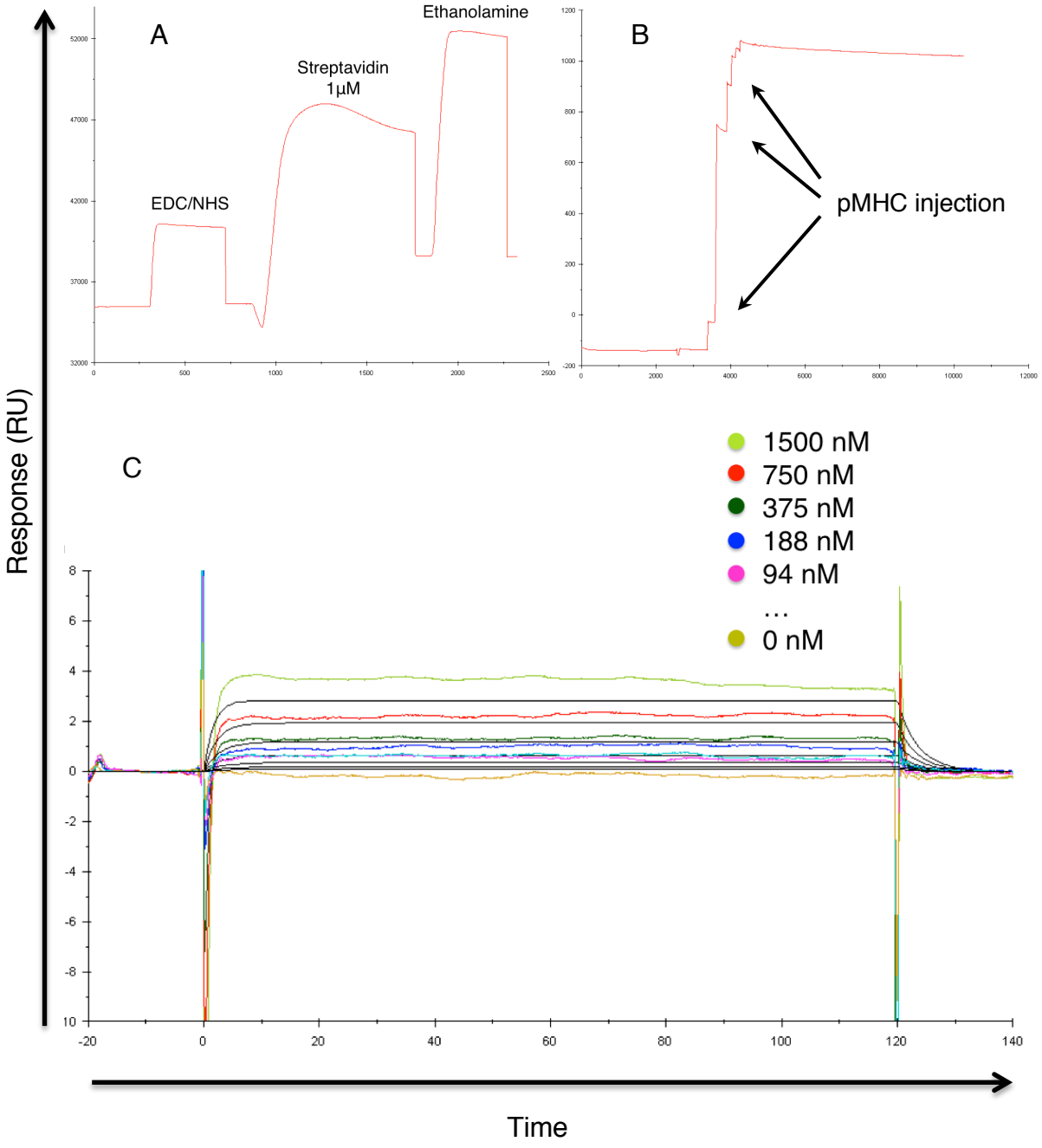

Figure 2-7. SPR characterization of anti-Mart1 Fn3. (A) Streptavidin is immobilized to the sensor chip by amine coupling. (B) Biotinylated HLA-A2-Mart1 is bound to the streptavidin chip to 1200 RUs. (C) Response following injections of increasing concentrations of anti-Mart1 Fn3 demonstrates dose-dependent binding.

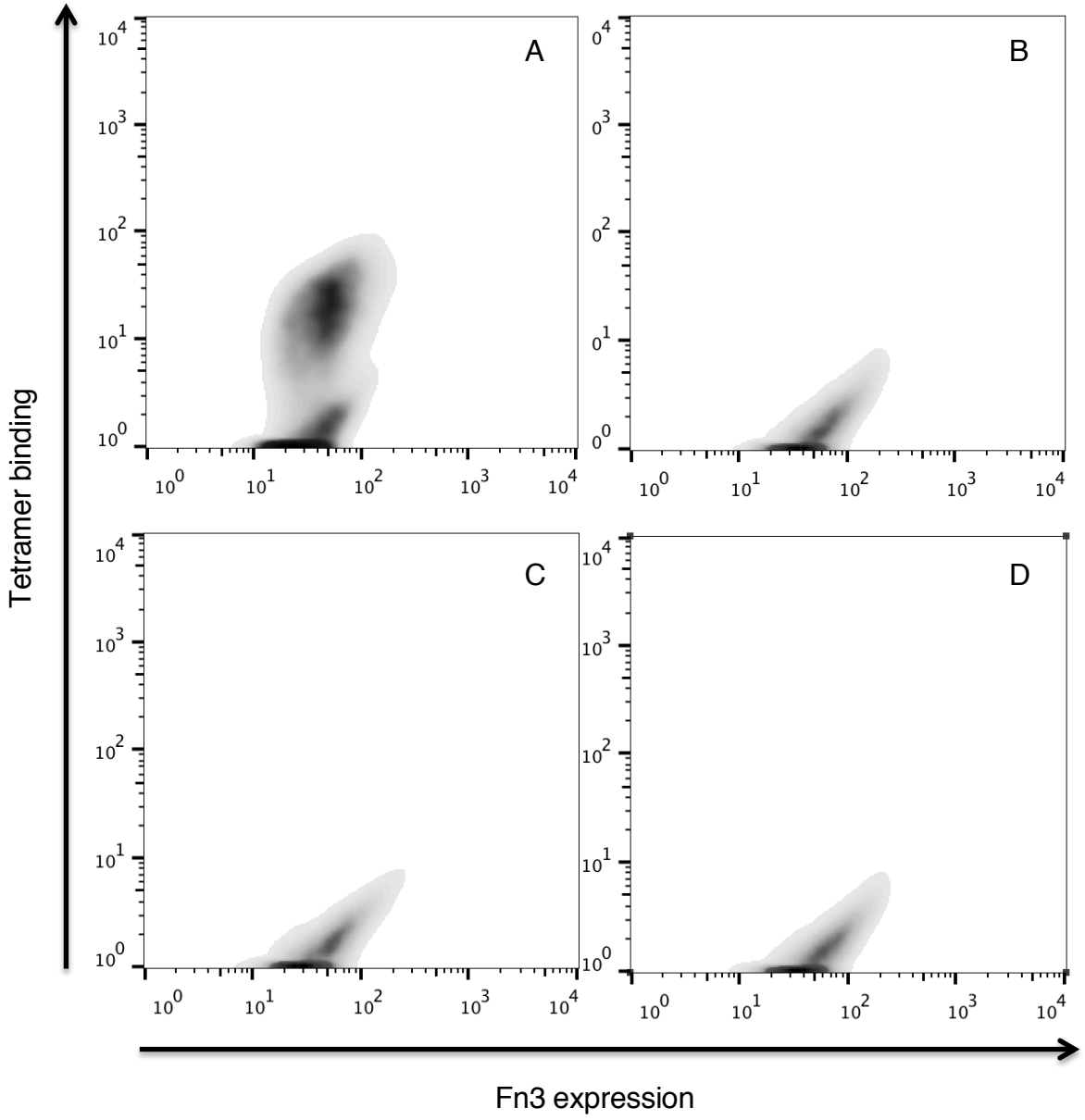

Figure 2-8. Reversions of anti-Mart1 Fn3 loops to their respective wild-type Fn3 sequence, evaluated for binding to HLA-A2-Mart1 by yeast display. The y-axis tracks binding to tetramer, while the x-axis reports Fn3 expression by c-myc staining. All clones express at similar levels. However, while (A) anti-Mart1 Fn3 binds HLA-A2-Mart1, reversions to wild-type (B) BC, (C) DE, and (D) FG Fn3 loops ablates binding to tetramer.

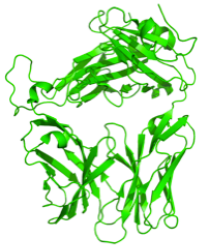

T-cell receptors

Pros
- Selective binding

Cons
- Low affinity
- Low stability/solubility
- Difficult to engineer in display

Naïve display libraries

Pros
- Can be used to screen for affinity/stability

Cons
- Difficult to select for peptide-specificity

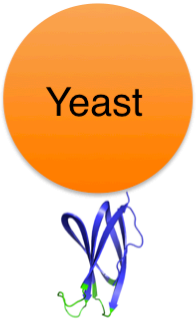

Fn3-TCR chimera

- Selective binding to target antigen
- Expresses in display
- Can be engineered for higher affinity and stability by established methods (i.e. we know what positions can be mutated)

Figure 2-9. Implications of this study for future efforts to engineer anti-pMHC, Fn3-based binders. Robust expression in yeast display and verified pMHC selectivity allow Fn3-TCR chimeras such as anti-Mart1 Fn3 to serve as starting scaffolds for further engineering.

References

1. Cole, D.K., et al., *Germ line-governed recognition of a cancer epitope by an immunodominant human T-cell receptor.* J Biol Chem, 2009. **284**(40): p. 27281–9.

2. Borbulevych, O.Y., et al., *TCRs Used in Cancer Gene Therapy Cross-React with MART-1/Melan-A Tumor Antigens via Distinct Mechanisms.* The Journal of Immunology, 2011. **187**(5): p. 2453–2463.

3. Bloom, L. and V. Calabro, *FN3: a new protein scaffold reaches the clinic.* Drug Discovery Today, 2009. **14**(19–20): p. 949–955.

4. Tolcher, A.W., et al., *Phase I and pharmacokinetic study of CT-322 (BMS-844203), a targeted Adnectin inhibitor of VEGFR-2 based on a domain of human fibronectin.* Clin Cancer Res, 2011. **17**(2): p. 363–71.

5. Hackel, B.J., A. Kapila, and K.D. Wittrup, *Picomolar affinity fibronectin domains engineered utilizing loop length diversity, recursive mutagenesis, and loop shuffling.* J Mol Biol, 2008. **381**(5): p. 1238–52.

6. Kimura, R.H., et al., *Engineered knottin peptides: a new class of agents for imaging integrin expression in living subjects.* Cancer Res, 2009. **69**(6): p. 2435-42.

7. Chao, G., et al., *Isolating and engineering human antibodies using yeast surface display.* Nat Protoc, 2006. **1**(2): p. 755-68.

8. Hoover, D.M. and J. Lubkowski, *DNAWorks: an automated method for designing oligonucleotides for PCR-based gene synthesis.* Nucleic Acids Res, 2002. **30**(10): p. e43.

9. Zaccolo, M., et al., *An Approach to Random Mutagenesis of DNA Using Mixtures of Triphosphate Derivatives of Nucleoside Analogues.* Journal of Molecular Biology, 1996. **255**(4): p. 589–603.

10. Gibson, D.G., *Enzymatic assembly of overlapping DNA fragments.* Methods Enzymol, 2011. **498**: p. 349-61.

11. Chao, G., et al., *Isolating and engineering human antibodies using yeast surface display.* Nat. Protocols, 2006. **1**(2): p. 755–768.

12. Kontermann, R. and S. Dübel, *Antibody Engineering: Volume 1*. 2010: Springer.

13. Baker, B.M. and D.C. Wiley, *αβ T Cell Receptor Ligand-Specific Oligomerization Revisited.* Immunity, 2001. **14**(6): p. 681–692.

14. Gibson, D.G., *Chapter fifteen - Enzymatic Assembly of Overlapping DNA Fragments*, in *Methods in Enzymology*, V. Christopher, Editor. 2011, Academic Press. p. 349–361.

15. Das, R. and D. Baker, *Macromolecular Modeling with Rosetta.* Annual Review of Biochemistry, 2008. **77**(1): p. 363–382.

16. Lewis, S.M. and B.A. Kuhlman, *Anchored Design of Protein-Protein Interfaces.* PLoS ONE, 2011. **6**(6): p. e20872.

17. Cota, E., et al., *The folding nucleus of a fibronectin type III domain is composed of core residues of the immunoglobulin-like fold.* Journal of Molecular Biology, 2001. **305**(5): p. 1185–1194.

18. Stewart-Jones, G., et al., *Rational development of high-affinity T-cell receptor-like antibodies.* Proc Natl Acad Sci U S A, 2009. **106**(14): p. 5784–8.

19. Asial, I., et al., *Engineering protein thermostability using a generic activity-independent biophysical screen inside the cell.* Nat Commun, 2013. **4**: p. 2901.

20. Rakestraw, J.A., et al., *Secretion-and-capture cell-surface display for selection of target-binding proteins.* Protein Eng Des Sel, 2011. **24**(6): p. 525–30.

21. Benatuil, L., et al., *An improved yeast transformation method for the generation of very large human antibody libraries.* Protein Eng Des Sel, 2010. **23**(4): p. 155–9.

22. Shusta, E.V., et al., *Directed evolution of a stable scaffold for T-cell receptor engineering.* Nat Biotechnol, 2000. **18**(7): p. 754–9.

Chapter 3

CONSTRUCTION AND SCREENING OF 4D5-TCR LIBRARIES ENABLES THE DISCOVERY OF PEPTIDE-MHC-SELECTIVE CLONES

Abstract

The relative success of the TCR-to-Fn3 domain swapping motivates the question of whether TCR binding domains may be successfully transferred to homologous scaffolds other than Fn3. The Fab fragment of antibodies is a particularly compelling candidate for such an investigation, because of its extensive validation as a molecular recognition scaffold, and because of its more faithful homology to the TCR framework. To this end, the 4D5 scaffold is selected as a target for binding domain transfer of HLA-A2-Mart1- and HLA-A2-Ny-Eso-1-specific TCRs. In order to rationally transfer the CDR loops of these TCRs to 4D5, a library assembly method was developed, guided by the previous TCR-to-Fn3 study and by established approaches for 4D5 loop diversification. Similar to the TCR-to-Fn3 study, successful transfer of binding properties entailed the construction of a mutagenized library. Subsequent screens and selections in yeast display led to the identification of clones selective for HLA-A2-Mart1 and HLA-A2-Ny-Eso-1. Expression and further characterization of the clones in soluble format demonstrated a reduction in yield and solubility relative to wild-type 4D5. However, binding measurements evaluated by surface plasmon resonance (SPR) affirmed the functionality of a Mart1-selective 4D5 variant. The findings of this study, concurrent with the implications of Chapter 2, suggest that the grafted TCR loops, while conferring binding selectivity, may also engender biophysical deficiencies.

Introduction

Chapter 2 provides a proof of concept for the domain transfer of paratopes from TCRs onto the homologous protein scaffold Fn3. Although Fn3 is a convenient molecular scaffold to implement as a target of TCR domain transfer, because of its high thermostability and purported ease of expression in *E. Coli*, these advantages did not transfer well to clones selected from a library derived from TCR loop sequences. Furthermore, while the contribution of the Vα domain of HLA-A2-Mart1-specific TCRs to peptide binding appears to be sufficient for transfer of selectivity to Fn3, the Vα and Vβ domains of TCRs both provide molecular contacts to the peptide epitope. Indeed, the Vα and Vβ domains are typically positioned to contact the N-terminal and C-terminal domains of the peptide within the MHC groove, respectively. Thus, in order to universally achieve TCR-like specificity, it may be important to utilize a scaffold that can acquire paratopes from both Vα and Vβ domains of TCRs.

The impact of TCR loop sequences on the solubility of Fn3 also underscores the importance of loop sequence on the biophysical properties of the scaffold. Although Fn3 has been used successfully to engineer binders against a variety of targets, thorough studies on the precise impact of loop mutations accumulated at different positions, and on the impact of loop length diversity, are needed [1]. It has further been demonstrated that many variants generated by diversification of the BC, DE, and FG loops have substantially reduced thermodynamic stability [2]. With more insight into what positions can tolerate sequence diversity, and to what extent, more robust Fn3 libraries can be constructed, which may yield clones with improved biophysical characteristics.

In contrast, the 4D5 framework, based on the trastuzumab Fab sequence, is an extensively validated scaffold for generating naïve libraries for molecular recognition [3]. Particularly, there is vast knowledge informing how libraries may be generated, guided by experimental data and by sequence diversity within the Fab gene family [4]. In Chapter 1, a rationale is proposed for 4D5 as a suitable scaffold for TCR binding domain transfer. Notably, homology of the variable light (V_L) and variable heavy (V_H) domains of 4D5 to the Vα and Vβ domains of TCRs, respectively, suggests that CDR grafting may endow 4D5 with the peptide specificity of TCRs. In Chapter 2, a library cloning method is described whereby sequence and length diversity can be introduced into certain loops of Fn3. By examining the homology of TCR loops to the 4D5 scaffold, and by exploiting existing

knowledge of mutagenic 4D5 libraries [5], the sequences of homologous loops may be targeted for replacement from TCRs onto the 4D5 framework sequence.

I chose to validate the approach of TCR-to-4D5 domain swapping by engineering binders against HLA-A2-Mart1$_{26-35}$ and HLA-A2-Ny-Eso-1$_{157-165}$. Specifically, HLA-A2-Mart1 is targeted by the TCRs MEL5 [6], DMF4, and DMF5 [7], and HLA-A2-NyEso-1 is targeted by the TCRs 1G4 and c58/c61 [8]. Libraries of 4D5 mutants containing loop grafts from these Mart1- and Ny-Eso-1-specific TCRs may be generated by adapting the polymerase chain reaction (PCR)-based assembly method implemented in Chapter 2. The techniques of yeast display and fluorescence activated cell sorting (FACS) may then enable the high-throughput screening and selection of positive binding clones.

Materials and Methods

Reagents and strains

The BirA-tagged and biotinylated extracellular domains of HLA-A2-Mart1 and HLA-A2-Ny-Eso-1 were provided by the NIH Tetramer Facility. Yeast display *Saccharomyces cerevisiae* strain EBY100, yeast display plasmid pPNL6, yeast secretion strain YVH10, and yeast secretion plasmid pPNL9 were obtained from Pacific Northwest National Laboratory. All yeast display protocols, buffers, and reagents were used as previously described [9, 10]. Oligonucleotides were obtained from Integrated DNA Technologies, and PCR assembly primers were designed using DNAWorks from NIH's Helix Systems [11]. Gene mutagenesis was performed by error-prone PCR as previously described [12], with nucleotide analogs from TriLink Biotechnologies. KOD Hot Start Polymerase from Novagen was used to PCR assemble gene inserts. The inserts have flanking 20-40 base pair overlaps with the desired cloning site in their respective, linearized plasmids. These were assembled into the appropriate plasmids using either yeast homologous recombination or Gibson cloning into TOP10 *Escherichia coli* cells. Reagents for Gibson cloning are as previously described [13], and constructs cloned into TOP10 competent cells were subsequently mini-prepped and transformed into yeast. Purification resins included HIS-select HF Nickel Affinity Gel from Sigma and StrepTactin Sepharose High Performance from GE Healthcare Life Sciences. Unless otherwise stated, all chemicals were from Sigma, and all *E. coli* strains from Life Technologies. Soluble protein expression was performed in 2.8 L glass culture flasks from Corning, using Freestyle 293 Expression Medium from Life Technologies. Protein was concentrated in Amicon 10,000 Da MWCO centrifugal filters from EMD Millipore. DNA extraction was performed with kits from Qiagen.

Loop grafts, error-prone mutagenesis, and library assembly

The 4D5 library was constructed to produce the wild-type sequence in the framework regions and to graft the CDR1α, CDR3α, CDR1β, CDR2β, and CDR3β sequences of HLA-A2-Mart1- and HLA-A2-Ny-Eso-1-specific TCRs to the CDR-L1, CDR-L3, CDR-H1, CDR-H2, and CDR-H3 loops of 4D5, respectively. In particular, two libraries were generated: one corresponding to grafts from Mart1-specific TCRs and the other to grafts from Ny-Eso-1-specific TCRs. Excision points for the loop grafts were determined by sequence alignment of 4D5 and TCR V-domains, using previously defined boundaries for 4D5 CDR diversification to appropriately demarcate the

loops (Figure 3-1). The DNA encoding for CDR-L1 residues 27-34 was replaced by DNA encoding for the CDR1α residues 27-38. Similarly, the DNA for CDR-L3 residues 91-97 was replaced by DNA encoding for the CDR3α residues 107-115; DNA for CDR-H1 residues 27-35 was replaced by DNA encoding for the CDR1β residues 27-38; DNA for CDR-H2 residues 50-59 was replaced by DNA encoding for the CDR2β residues 55-67; DNA for CDR-H3 residues 99-109 was replaced by DNA encoding for the CDR3β residues 107-117. All residue numbers for TCRs correspond to the IMGT numbering designated for TRAV gene sequences, and residue numbers for 4D5 correspond to indexing used in the PDB file 1n8z, utilizing the Chothia numbering scheme [14]. Double-stranded DNA corresponding to these loop fragments (with 30 base pairs of homology to adjoining framework regions), as well as double-stranded DNA corresponding to the constant framework regions, were prepared from pairs of complementary oligonucleotides by overlap extension PCR. The full-length 4D5 library was assembled by extension of a previously described protocol [2], by adapting the assembly of the Fn3 gene from seven overlapping fragments to the assembly of the 4D5 gene from eleven overlapping fragments. Each library assembled resulted in a theoretical library size of approximately 1000 unique clones of 4D5-TCR chimeras.

Error-prone PCR directed solely at the solvent-exposed loops of these libraries was used to focus diversity on the likely paratope. 4D5 genes were constructed with conserved wild-type framework sequence and randomly mutated loops from the pool of 4D5-TCR chimeras assembled above. For each library, error-prone PCR of the loop regions was performed via five separate 50 μL reactions with 20 mM 8-oxo-deoxyguanosine triphosphate and 20 mM 2'-deoxy-p-nucleoside-5'-triphosphate and primers flanking the diversified CDR loops. The reaction mixtures were denatured at 94°C for 3 min, cycled 15 times at 94°C for 45s, 60°C for 30s, and 72°C for 90s, and finally extended at 72°C for 10 min. Multiple preliminary mutagenesis reactions of the wild-type plasmid were conducted at different nucleotide analog concentrations. Sequence analysis and comparison to a wild-type framework indicated the aforementioned conditions yield one to five amino acid mutations per loop. The PCR products were purified by agarose gel electrophoresis and each amplified in four 100-μL PCR reactions containing 1× Taq buffer, 2 mM MgCl2, 1 μM of each primer, 0.2 mM (each) dNTPs, 4 μL of error-prone PCR product (of 40 μL from gel extraction), and 2.5 U of Taq DNA polymerase. The reactions were thermally cycled at the same conditions except that 35 cycles were used. The full-length 4D5 libraries were then assembled

from the mutagenized loop fragments and constant framework fragments similarly to the non-mutagenized library above.

Yeast display, flow cytometry, and sorting

Yeast displayed protein was expressed at 20ºC and 250 RPM for 16 hours. Displayed protein was incubated with biotinylated monomeric HLA-A2-Mart1 or HLA-A2-Ny-Eso-1, or tetrameric peptide-MHC prepared by incubating streptavidin–fluorophore (R-phycoerythrin, AlexaFluor488; Invitrogen, Carlsbad, CA) with biotinylated pMHC in a 1:4 ratio (four equal additions of fluorophore, 10 min in between additions, covered from light at room temperature) in phosphate-buffered saline (PBS). Flow cytometry was performed on a BD Biosciences FACSCalibur, and data was analyzed with FlowJo from Tree Star. 50,000 cell counts were collected for binding analysis experiments. All yeast display experiments were performed in PBS with 0.1% w/v bovine serum albumin (PBSF) buffer as previously described [15]. Libraries were constructed by high efficiency yeast electroporation [10]. FACS was performed on the MoFlo XDP instrument from Beckman Coulter using polypropylene BD Falcon FACS tubes.

Protein L Selection

Magnetic protein L beads were produced using biotinylated protein L (Pierce) and magnetic streptavidin Dynabeads (Invitrogen). Specifically, 33 pmoles of biotinylated protein L was combined with 4×10^6 beads and 100 μL of PBSF and nutated at 4ºC for 1 hour. Magnetic beads were separated in a magnetic separation rack (New England Biolabs), and washed twice with PBSF. The protein L beads were then used to select for yeast expressing 4D5 clones that bind to protein L, using a magnetic bead selection method described previously [16, 17].

Measurement of K_d in yeast display

Affinity titrations to determine the equilibrium dissociation constant (K_d) for given clone were performed as previously described [17]. All incubations were performed while nutating at room temperature. Quenched samples were placed on ice in a 4ºC cold room. All work with cold samples was performed at 4ºC with chilled tips and a dedicated cold room centrifuge. Samples were handled in 1.5 mL Eppendorf tubes, and then transferred to a Nunc polypropylene 96-well V-bottom plate prior to addition of secondary reagents for ease of handling and standardization between samples.

Prior to flow cytometry analysis, samples were spun down and kept as pellets on ice, covered from light. Immediately prior to analysis, individual samples were resuspended in 0.5 mL of PBSF and transferred to a polystyrene BD Falcon FACS tube for loading. 20,000 cell counts were collected for each sample in kinetic assays. Analysis was performed in GraphPad Prism version 6.0d for OSX 10.9 from GraphPad Software. K_d was fit to the Michaelis-Menten model.

Expression of soluble anti-Mart1 and anti-Ny-Eso-1 4D5

4D5 clones were expressed in HEK293-6E mammalian secretion culture. The full light chain and Fab heavy chain sequence were subcloned separately into the mammalian expression vector pTT5 (NRC Biotechnology Research Institute), with a C-terminal hexa-histidine tag on the heavy chain. The heavy chain and light chain vectors were mixed at a 1:1 ratio by mass, and the corresponding proteins were expressed transiently in suspension HEK 293-6E cells (NRC Biotechnology Research Institute) using BioT transfection reagent (Bioland Scientific). Specfically, 1 mg of combined DNA was added to 34 mL of sterile filtered PBS in a 50 mL canonical tube and mixed thoroughly, after which 1 mL of BioT was added. The mixture was briefly vortexed and added to 1 L of culture supernatant.

Prior to transfection, cells are grown until they reach a density of 2×10^6 cells/mL, and are split to a density of 1×10^6 cells/mL immediately preceding transfection. Cultures are grown at 8% CO_2, 37ºC, 90 RPM, humidified atmosphere for 6 days after transfection. Pellets were spun down and discarded twice, and the supernatant was sterile filtered and loaded onto HIS-select resin. After washing with the same buffer, samples were eluted in elution buffer (300 mM NaCl, 20 mM sodium phosphate, pH 7.8, 0.05% tween 20, 2.5% glycerol, 200 mM imidazole), concentrated, and run over an analytical Superdex-75 column from Amersham Pharmacia on the ÄKTA FPLC system. Sample volume was 0.5 mL, run at 0.5 mL/min in PBS. Typical yields were 0.2 mg/L from mammalian secretion culture.

Characterization of soluble anti-Mart1 4D5 by surface plasmon resonance

Surface plasmon resonance (SPR) experiments were performed as previously described [18] using a Biacore T200 instrument with CM5 sensor chips and HBS-EP$^+$ buffer (GE Healthcare) at 25°C. Streptavidin was first coupled to the sensor surface using amine coupling, and biotinylated HLA-A2-Mart1 was then immobilized at different densities to flow cells 2 through 4 of the

streptavidin coated chip. Soluble Fab was flowed over the chip at twofold serial dilutions ranging from 9000 nM to 70 nM, with a buffer-only control to establish a baseline. Data were corrected for bulk solvent effects using a flow cell containing immobilized streptavidin only. Flow rates were 5 μl/min. Data were processed with Biacore T200 Evaluation Software (GE Healthcare).

Results

Identification of dominant clones

The error-prone libraries of 4D5 genes were incorporated into a yeast surface display system by homologous recombination with the pPNL6 vector incorporating an N-terminal Aga2 protein for display on the yeast surface and a C-terminal c-myc epitope for detection of full-length 4D5. Library transformation yielded 3×10^7 yeast transformants per library. Library sizes of 3×10^8 per library were expressed and subjected to five sequential fluorescence-activated cell sorting (FACS) sorts with decreasing concentrations of HLA-A2-Mart1 tetramer or HLA-A2-Ny-Eso-1 tetramer on the Mart1- and Ny-Eso-1-directed libraries, respectively. Sorting against 200 nM for the first two sorts and 100 nM for the final three sorts, the top 1-5% of each population for both antigen binding and c-myc expression levels was collected for culture outgrowth. Diversity of each round was monitored by sequencing 10 clones at each step. By round five, each library converged upon a dominant clone with the CDR loop sequences reported in Table 3-1. Although the clone isolated from HLA-A2-Ny-Eso-1 selection corresponds to a full-length 4D5 product, the dominant clone isolated from HLA-A2-Mart1 selection corresponds to a gene construct comprising only the V_H domain of 4D5. This V_H-only gene product is likely the result of excision of the V_L segment and re-annealing to homologous Gly_4/Ser linker-encoding regions that are present both upstream of the V_L sequence and between the V_L and V_H sequences. This excision may have occurred in a subset of the clones through either the Gibson assembly step or yeast homologous recombination, during which constituent or endogenous exonucleases are capable of digesting the entire V_L sequence.

In order to isolate V_L-containing 4D5 variants binding to HLA-A2-Mart1, the first round of the library was re-expressed and subjected to alternating rounds of protein L magnetic bead selection and FACS sorting with HLA-A2-Mart1 tetramer. After four total additional rounds of selection, a full-length 4D5 variant was isolated (Table 3-1).

Notably, the CDR-H3 sequences of the full-length clones Ny.1 and Ma.2 contain no mutations and a single mutation relative to the CDR3β of parental TCRs, respectively, indicative of strong selective preference for the wild-type loop sequence. The CDR-H3 of antibodies is generally believed to play a dominant role in antigen recognition relative to other CDRs, inferred by the extent of sequence variability in natural antibodies and an abundance of structural information

revealing its contribution to interactions with antigen [19]. The conservation of wild-type TCR sequences in the CDR-H3 loops thus insinuates that the binding modes of these clones are similar to that of their parental TCRs.

Binding and selectivity of engineered 4D5 variants in yeast display

Yeast displaying Ny.1, Ma.1h, and Ma.2 were incubated with 100 nM HLA-A2-Mart1 tetramer or 100 nM HLA-A2-Ny-Eso-1 tetramer to determine the relative affinity of the clones to the same MHC allele presenting two different peptides. At this concentration of tetramer, Ny.1 exhibits clear binding to HLA-A2-Ny-Eso-1 and no detectable binding to irrelevant antigen (Figure 3-2). Similarly, Ma.1h exhibits clear binding to HLA-A2-Mart1 and no detectable binding to irrelevant antigen (Figure 3-2). These data suggest that both clones are peptide selective. In contrast, Ma.2 exhibits weak binding to HLA-A2-Mart1 that is qualitatively greater than the detected binding to HLA-A2-Ny-Eso-1. The computed mean fluorescence intensity (MFI) of the positively stained population is approximately 30% higher for HLA-A2-Mart1 tetramer than the same concentration of HLA-A2-Ny-Eso-1 tetramer (MFI of 14.1 and 10.8, respectively).

Affinity titrations were performed to determine the K_d at equilibrium for the three clones. Yeast displaying Ny.1 was incubated with varying concentrations of HLA-A2-Ny-Eso-1 tetramer (0–2000 nM) for two hours, and yeast displaying Ma.1h, and Ma.2 were incubated with varying concentrations of HLA-A2-Mart1 tetramer (0–2000 nM) for two hours. This experiment is not designed to determine the monovalent binding to pMHC antigens, as antigen is multivalently coupled to streptavidin-fluorophore (maximum valency of four). However, the binding affinities to cognate pMHC tetramer were measured to be 377 ± 86 nM for Ny.1, and 1088 ± 20 nM for Ma.2 (Figure 3-3).

Characterization of soluble Ma.2 by surface plasmon resonance

To confirm that the engineered 4D5 variants functions outside of display format, HEK293-6e cells were used as a host to express and secrete Ny.1 and Ma.2 in Fab format into the culture medium. Although Ny.1 did not express at appreciable yields in the culture supernatant, Ma.2 did express at quantifiable yields. Soluble Ma.2 Fab runs at a size consistent with that of a full-length Fab by comparison to FPLC standards (Figure 3-4).

The purified protein was subsequently characterized for binding to HLA-A2-Mart1 monomer by surface plasmon resonance. Streptavidin was first coupled to the sensor chip, and was followed by binding of biotinylated HLA-A2-Mart1 monomer, as described in Chapter 2. Varying concentrations of Ma.2 Fab were injected in order to obtain a binding isotherm and determine equilibrium dissociation. However, such a determination was not possible because binding was not measured at sufficiently high concentrations of Ma.2. Furthermore, whenever quantities of Ma.2 were reduced in volume to a concentration exceeding the upper limit of this experiment, a visible precipitate materializes, and concentration does not increase as measured by absorbance at 280 nm. This observation suggests that Ma.2 Fab is not well soluble in PBS. Nevertheless, the SPR data does demonstrate binding of soluble Ma.2 Fab to HLA-A2-Mart1, and that this binding exhibits a concentration dependence (Figure 3-5). Furthermore, the SPR trace qualitatively demonstrate that the binding kinetics exhibit a fast on-rate and fast off rate, which are analogous to the kinetics of association and dissociation of the wild-type DMF5 TCR [7], suggesting a potentially similar mechanism of binding for the two molecules.

Discussion

The 4D5 scFv framework is well established as a scaffold for library generation and for molecular recognition to a variety of targets [5]. Moreover, such engineering has led to the identification of soluble targeting molecules demonstrating satisfactory biophysical profiles [20]. The multitude of work in engineering the scaffold has yielded standardized methods for introducing diversity into the various CDR loops. Additionally, 4D5 is widely used as a scaffold for the grafting of murine antibody sequences, validating its utility as a target for domain transfer [21]. 4D5 is, in principle, a canonical scaffold target for TCR domain transfer, as the close homology of the Fab and TCR scaffolds suggest that CDR loops may be transferred in a way that preserves the integrity of the binding domain. However, the relatively low thermodynamic stability of scFv scaffolds may adversely affect the evolvability of the domain in the context of TCR binding domain transfer [22]. In particular, the proportion of clones exhibiting acceptable solubility and thermodynamic stability may diminish considerably as broader diversity is introduced into the loop regions [23].

The deleterious effect of extensive loop modifications on the biophysical characteristics of engineered 4D5 variants is evidenced by the low expression yields of clones Ny.1 and Ma.1h, and by the poor solubility of Ma.2. In effect, despite their demonstrated expression and selective binding to cognate peptide-MHC antigens in yeast display format, these molecules have limited use as soluble reagents. The introduction of non-native TCR loop sequences onto the framework of 4D5 may prompt the loss of solubility and expression of Ma.2 by a variety of mechanisms. For instance, a decrease in thermodynamic stability may arise from loop graft sequences driving the energetics of Ma.2 protein folding or dynamics from the native 4D5 conformation toward an aggregation-prone state. The TCR sequences may provoke such instability generally, or specifically within the context of the atypical 4D5 framework; the latter account is more likely in light of the reported soluble expression of the DMF5 TCR [7]. For instance, unfavorable interactions, particularly among CDR-L3 and CDR-H3 residues, may disrupt the 4D5 V_H-V_L interface and expose hydrophobic patches, triggering aggregation [24]. Conversely, loss in solubility may also result from the presence of sequence epitopes within Ma.2 loops that promote nonspecific interactions, although this is less probable given the sequences are derived from a palpably well-behaved TCR. Although in Chapter 2, purification of soluble anti-Mart1 Fn3 revealed the likely presence of a soluble oligomeric state, the FPLC chromatogram of Ma.2

indicates a single species corresponding to the 4D5 Fab (Figure 3-4). Accordingly, the poor solubility of Ma.2 may arise from a different mechanism than that causing the poor solubility of anti-Mart1 Fn3. These finding affirm that, although solvent-exposed loops of scaffolds such as 4D5 and Fn3 are generally tolerant of diverse sequences, modifications of such domains may unexpectedly impair the general biophysical fitness of these proteins [25].

In addition to poor solubility, Ma.2 exhibits an apparently low affinity for HLA-A2-Mart1. Such weak binding may be attributed to the fact that the putative binding domain of Ma.2 is derived from the DMF5 TCR, which binds to HLA-A2-Mart1 with a K_d of 6 μM [7]. By itself, the low binding affinity of a 4D5 variant is quite surmountable, as additional rounds of focused or random mutagenesis may improve the affinity by several orders of magnitude [2]. Indeed, such engineering is feasible for the 4D5 scaffold due to its pronounced expression in yeast display format, which enables the continued enrichment of higher affinity clones from mutagenized libraries. However, the lack of selective pressure on the library for adequate expression yields and solubility may perpetuate the selection of clones exhibiting undesirable biophysical characteristics.

In future studies, selection methods that incorporate a selective pressure or concurrent screen for protein solubility will be critical to attaining engineered variants that are useful as soluble reagents. Secretion-and-capture yeast display, in which a 4D5 library could be secreted by the host yeast strain before being anchored to the yeast cell wall by a strong, non-covalent interaction, is an example of such a system [26]. Another potential route would be to establish spatial separation of single yeast cells secreting individual 4D5 clones, namely by using a microfluidic device in which individual chambers contain immobilized antigen, before screening for binding of single clones [27, 28]. Such microfluidic techniques have been used, for example, in the profiling of cytokine secretions from primary T cells, and allow up to 10^4 cells per experiment to be evaluated [29, 30]. In both cases, the protein of interest must be solubly secreted before binding may be assayed, requiring a protein to remain stable in solution in order to endure selection; as a result, such methods are more likely to effect efficient conversion to soluble production formats.

Concurrent with a more appropriate selection system, the execution of TCR-to-4D5 binding domain transfer may also benefit from the screening of larger libraries, permitting the inspection

of a greater breadth of sequence space. Specifically, library size may be enlarged either by increasing the throughput of yeast transformations or by implementing optimized transformation protocols [31]. Furthermore, integrating a more exhaustive mutagenesis scheme, such as whole gene error-prone PCR [2], may yield libraries consisting of stabilizing framework mutations that may compensate for destabilizing loop modifications. Although the number of transformants screened in this study (3×10^7) is considerable, the apparent presence of V_L-only or V_H-only domains resulting from yeast homologous recombination may markedly diminish the functionality of the library. By increasing the size of the library, we may similarly increase the putative number of soluble binders in the library that may be enriched. Thus, a more populous library universally improves the likelihood of discovering biophysically superior 4D5 variants.

Conclusion

The findings of this study demonstrate that engineered 4D5 clones isolated from libraries of diversified 4D5-TCR chimeras exhibit TCR-like peptide selectivity against the selected antigens HLA-A2-Mart1 and HLA-A2-Ny-Eso-1. Importantly, these results suggest that the binding domains of TCRs can be transferred to the 4D5 scaffold such that the resulting libraries express efficiently in yeast display, in contrast to the TCRs from which the libraries are derived [32]. Although synthetic and pre-immune 4D5 libraries may be used to select against pMHC antigens, ensuing hits are unlikely to possess TCR-like peptide selectivity, given the myriad immunodominant epitopes of HLA-A2 and diverse binding modes that can be accommodated [33]. In contrast, constructing libraries by transplanting the binding domains of well-validated, peptide-selective TCRs likely predisposes library clones toward TCR-like binding modes. Moreover, although TCRs are generally refractory to display formats and are thus challenging to engineer, selected 4D5 variants, such as Ny.1 and Ma.2, are demonstrably amenable to yeast display selection. Consequently, such clones may be further engineered for greater affinity and, with suitable methods, for improved solubility. In particular, constructing larger libraries, and using technologies such as secretion-and-capture yeast display or high-throughput, single-cell microarrays increases the number of evaluable hits and the likelihood that such hits can be solubly expressed, respectively. Therefore, such approaches are expected to improve the chances of future efforts exploiting the TCR-to-4D5 methodology to attain soluble reagents with TCR-like selectivity for pMHC antigens.

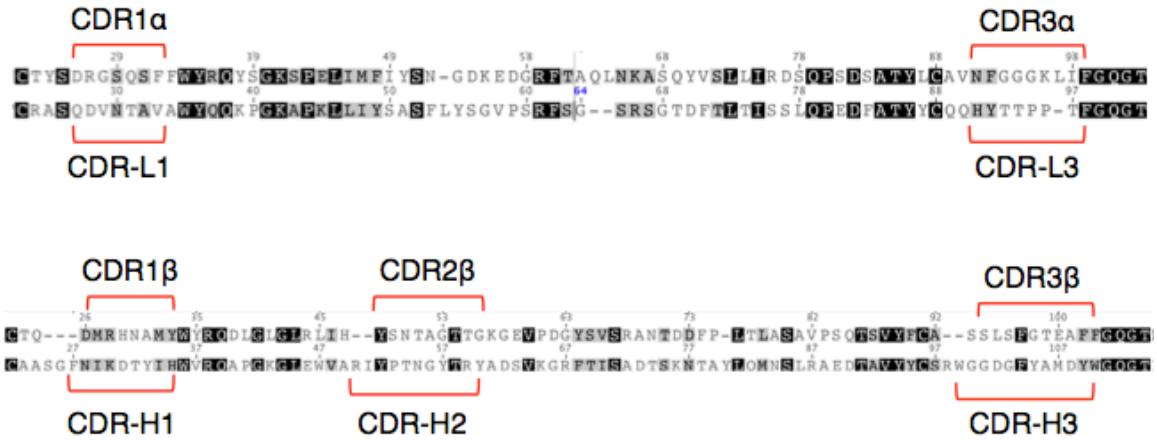

Figure 3-1. Pairwise sequence alignment of 4D5 and T cell receptor V-regions. (A) DMF5 TCR Vα domain (top) aligned to 4D5 V_L (bottom). (B) DMF5 TCR Vβ domain (top) aligned to 4D5 V_H (bottom).

A

Loop	Sequence	Source TCR	WT TCR sequence	WT 4D5 sequence
CDR-L1	-	-	-	-
CDR-L3	-	-	-	-
CDR-H1	MRHGAIH	TCR DMF5	MRHNAMY	FNIKDTYIH
CDR-H2	WSSAAGTTR	TCR DMF5	YSNTAGTTG	RIYPTNGYTR
CDR-H3	PWSFGTEAL	TCR DMF5	SLSFGTEAF	WGGDGFYAMDY

B

Loop	Sequence	Source TCR	WT TCR sequence	WT 4D5 sequence
CDR-L1	GRGSQS	TCR DMF5	DRGSQS	QDVNTA
CDR-L3	DPGGGKLT	TCR DMF5	NFGGGKLI	HYTTPPT
CDR-H1	FNHNAMY	TCR DMF5	MRHNAMY	FNIKDTYIH
CDR-H2	YSNAAGATG	TCR DMF5	YSNTAGTTG	RIYPTNGYTR
CDR-H3	SLSFGTEAS	TCR DMF5	SLSFGTEAF	WGGDGFYAMDY

C

Loop	Sequence	Source TCR	WT TCR sequence	WT 4D5 sequence
CDR-L1	QYAIYDLR	TCR 1G4	SAIYNLQ	QDVNTAVA
CDR-L3	RSLLDGTHTP	TCR c58/c61	RPLLDGTYIP	HYTTPP
CDR-H1	VNHGYIH	TCR 1G4	MNHEY	FNIKDTYIH
CDR-H2	YPVDAGITD	TCR 1G4	YSVGAGITD	RIYPTNGYTR
CDR-H3	SYVGNTGELF	TCR 1G4	SYVGNTGELF	WGGDGFYAMDY

Table 3-1. Loop sequences of dominant clones (A) Ma.1h, (B) Ma.2, and (C) Ny.1. Amino acids that differ relative to the parental TCR sequence (resulting from error-prone PCR) are highlighted in red. Positions that revert to the amino acid identity of wild-type Fn3 are highlighted in blue.

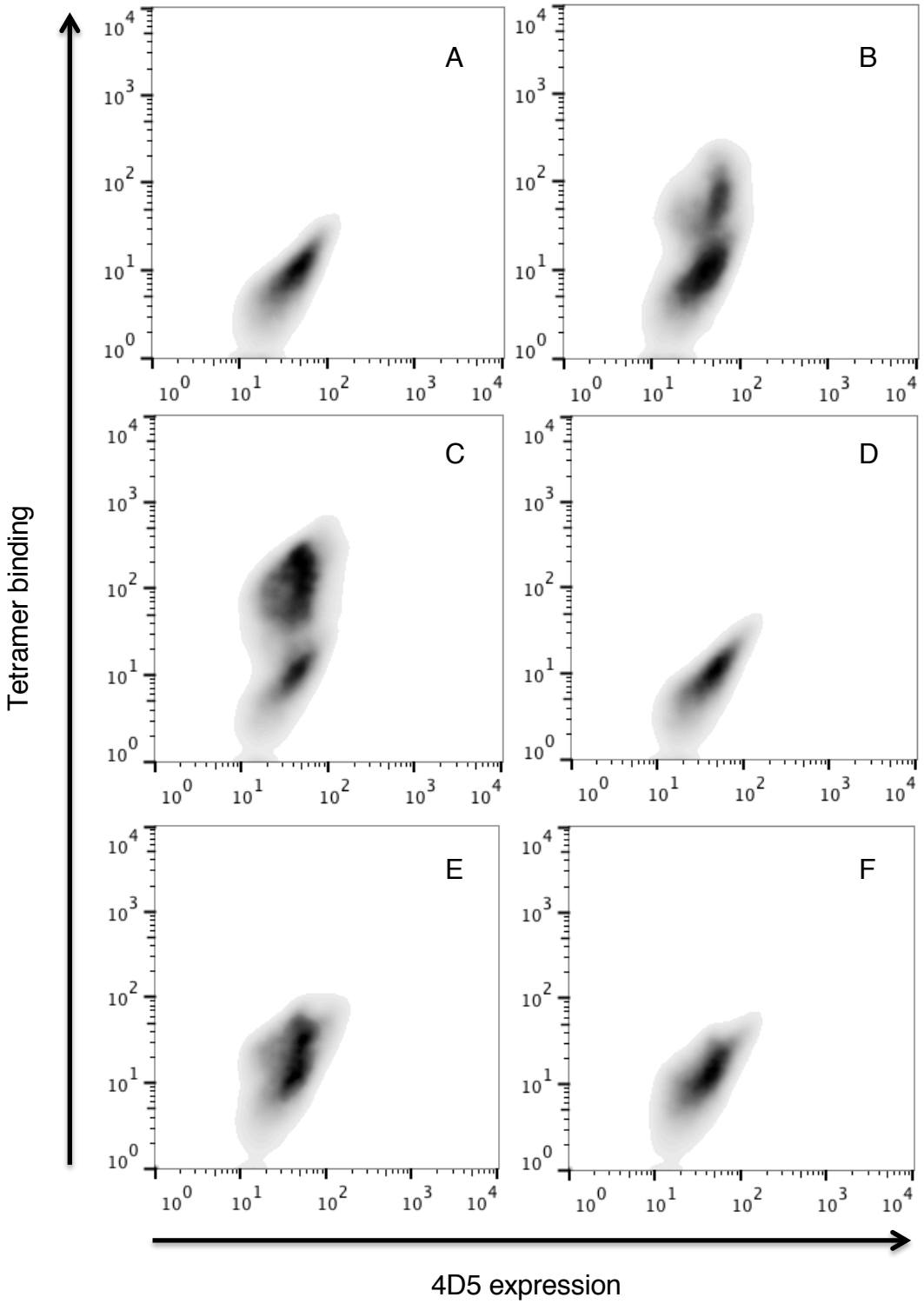

Figure 3-2. FACS plots demonstrating the selectivity of various engineered 4D5 variants for cognate pMHC antigen in yeast display. Ny.1 exhibits no apparent binding for (A) HLA-A2-Mart1, yet binds positively to (B) HLA-A2-Ny-Eso-1. Ma.1h selectively binds to (C) HLA-A2-Mart1 over (D) HLA-A2-Ny-Eso-1. Ma.2 binds appreciably more to (E) HLA-A2-Mart1 than to (F) HLA-A2-Ny-Eso-1.

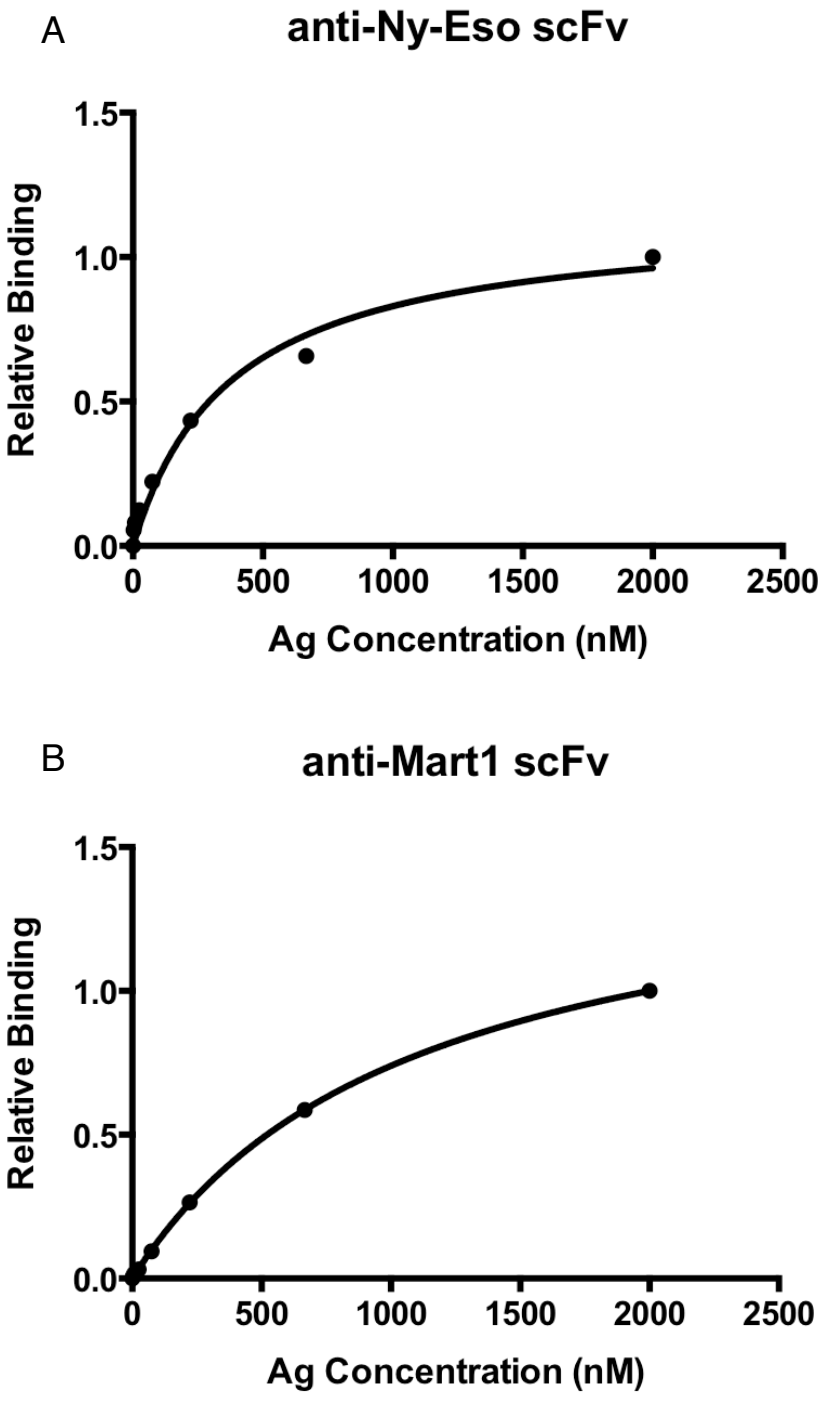

Figure 3-3. Equilibrium affinity titration of (A) HLA-A2-Ny-Eso-1 tetramer against yeast displayed Ny.1, and (B) HLA-A2-Mart1 tetramer against displayed Ma.2.

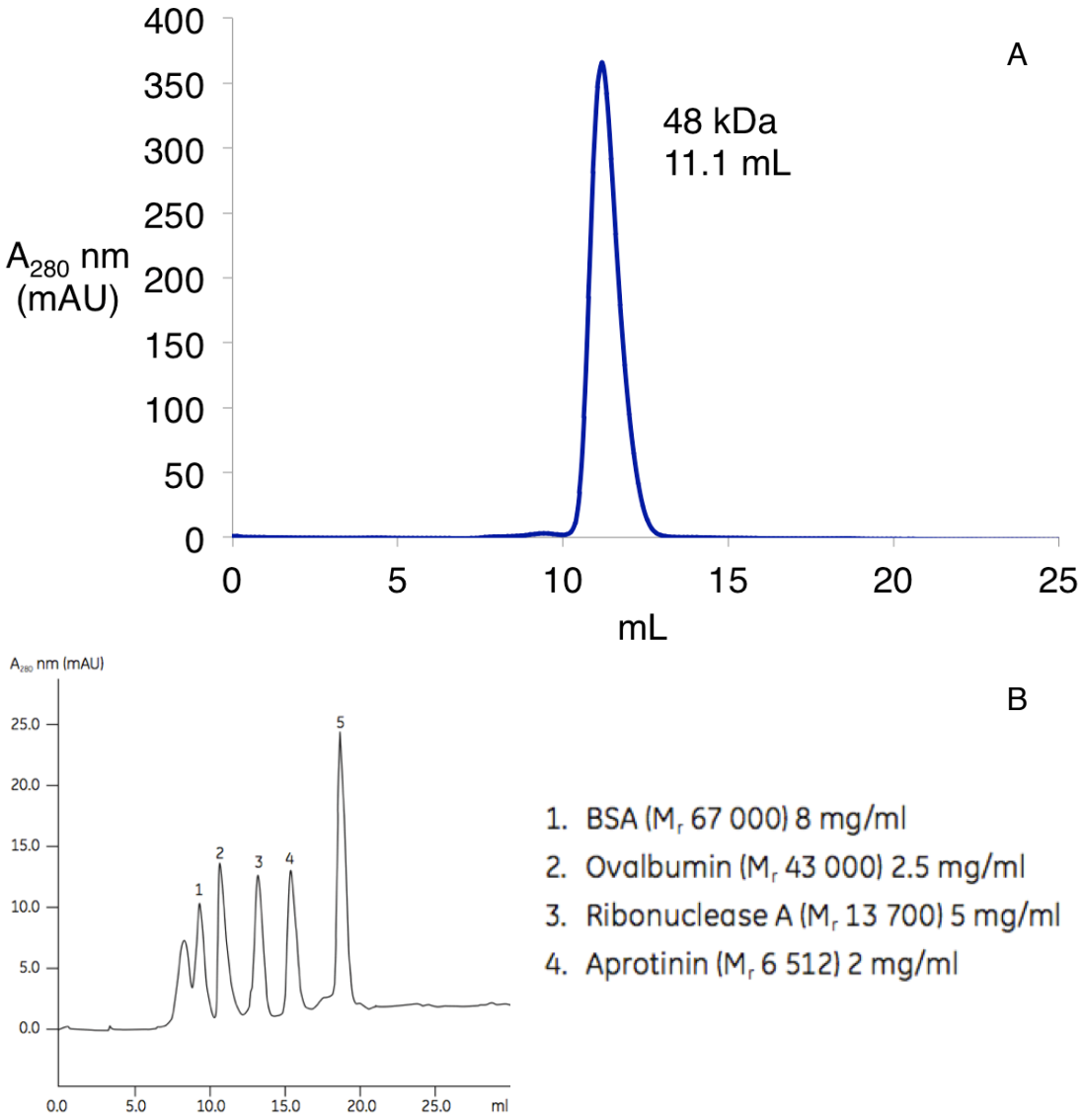

Figure 3-4. (A) Gel filtration profile of soluble Ma.2 Fab. The single, prominent corresponds to the expected size of the engineered 4D5 Fab. (B) Standards from the AKTA manual for comparison.

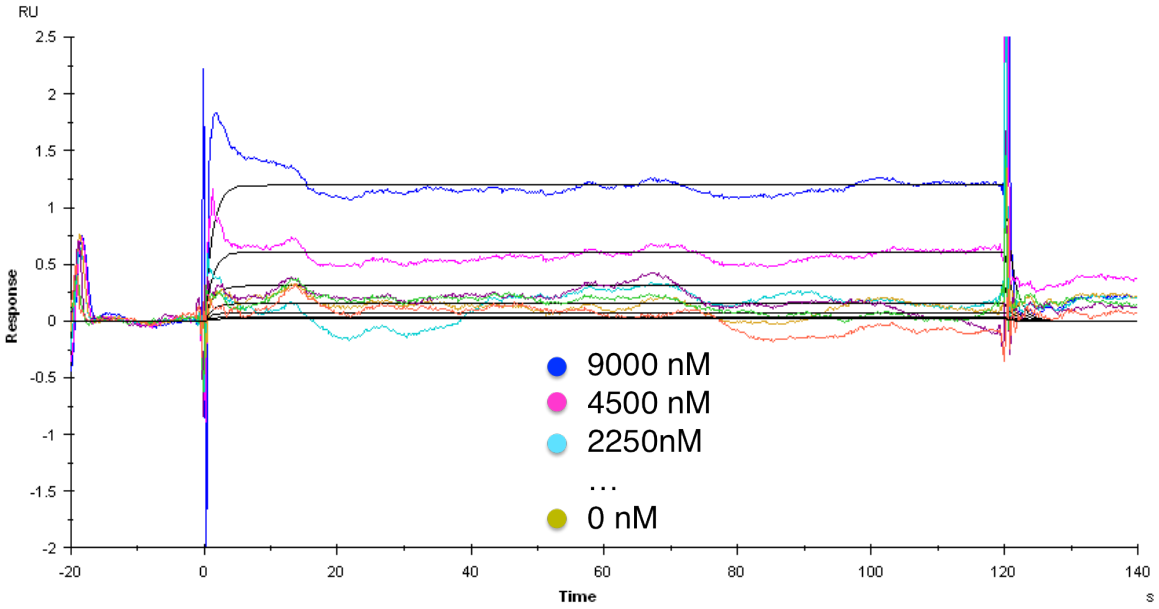

Figure 3-5. SPR characterization of soluble Ma.2 Fab. Response following injections of increasing concentrations of Ma.2 Fab demonstrates dose-dependent binding, although clearly apparent only for the two highest concentrations of Ma.2 assayed.

References

1. Hackel, B.J., et al., *Stability and CDR composition biases enrich binder functionality landscapes.* J Mol Biol, 2010. **401**(1): p. 84–96.

2. Hackel, B.J., A. Kapila, and K.D. Wittrup, *Picomolar affinity fibronectin domains engineered utilizing loop length diversity, recursive mutagenesis, and loop shuffling.* J Mol Biol, 2008. **381**(5): p. 1238–52.

3. Bostrom, J. and G. Fuh, *Design and construction of synthetic phage-displayed Fab libraries.* Methods Mol Biol, 2009. **562**: p. 17–35.

4. Sidhu, S.S., et al., *Phage-displayed antibody libraries of synthetic heavy chain complementarity determining regions.* J Mol Biol, 2004. **338**(2): p. 299–310.

5. Fellouse, F.A., et al., *High-throughput generation of synthetic antibodies from highly functional minimalist phage-displayed libraries.* J Mol Biol, 2007. **373**(4): p. 924–40.

6. Cole, D.K., et al., *Germ line-governed recognition of a cancer epitope by an immunodominant human T-cell receptor.* J Biol Chem, 2009. **284**(40): p. 27281–9.

7. Borbulevych, O.Y., et al., *TCRs Used in Cancer Gene Therapy Cross-React with MART-1/Melan-A Tumor Antigens via Distinct Mechanisms.* The Journal of Immunology, 2011. **187**(5): p. 2453–2463.

8. Zhao, Y., et al., *High-affinity TCRs generated by phage display provide CD4+ T cells with the ability to recognize and kill tumor cell lines.* J Immunol, 2007. **179**(9): p. 5845–54.

9. Kimura, R.H., et al., *Engineered knottin peptides: a new class of agents for imaging integrin expression in living subjects.* Cancer Res, 2009. **69**(6): p. 2435-42.

10. Chao, G., et al., *Isolating and engineering human antibodies using yeast surface display.* Nat Protoc, 2006. **1**(2): p. 755-68.

11. Hoover, D.M. and J. Lubkowski, *DNAWorks: an automated method for designing oligonucleotides for PCR-based gene synthesis.* Nucleic Acids Res, 2002. **30**(10): p. e43.

12. Zaccolo, M., et al., *An Approach to Random Mutagenesis of DNA Using Mixtures of Triphosphate Derivatives of Nucleoside Analogues.* Journal of Molecular Biology, 1996. **255**(4): p. 589–603.

13. Gibson, D.G., *Enzymatic assembly of overlapping DNA fragments.* Methods Enzymol, 2011. **498**: p. 349-61.

14. Chothia, C., et al., *Conformations of immunoglobulin hypervariable regions.* Nature, 1989. **342**(6252): p. 877–83.

15. Chao, G., et al., *Isolating and engineering human antibodies using yeast surface display.* Nat. Protocols, 2006. **1**(2): p. 755–768.

16. Ackerman, M., et al., *Highly avid magnetic bead capture: an efficient selection method for de novo protein engineering utilizing yeast surface display.* Biotechnol Prog, 2009. **25**(3): p. 774–83.

17. Kontermann, R. and S. Dübel, *Antibody Engineering: Volume 1*. 2010: Springer.

18. Baker, B.M. and D.C. Wiley, *αβ T Cell Receptor Ligand-Specific Oligomerization Revisited.* Immunity, 2001. **14**(6): p. 681–692.

19. Xu, J.L. and M.M. Davis, *Diversity in the CDR3 region of V(H) is sufficient for most antibody specificities.* Immunity, 2000. **13**(1): p. 37–45.

20. Rouet, R., et al., *Expression of high-affinity human antibody fragments in bacteria.* Nat Protoc, 2012. **7**(2): p. 364–73.

21. Jung, S. and A. Pluckthun, *Improving in vivo folding and stability of a single-chain Fv antibody fragment by loop grafting.* Protein Eng, 1997. **10**(8): p. 959–66.

22. Bloom, J.D., et al., *Protein stability promotes evolvability.* Proc Natl Acad Sci U S A, 2006. **103**(15): p. 5869–74.

23. Brockmann, E.C., *Selection of stable scFv antibodies by phage display.* Methods Mol Biol, 2012. **907**: p. 123–44.

24. Rothlisberger, D., A. Honegger, and A. Pluckthun, *Domain interactions in the Fab fragment: a comparative evaluation of the single-chain Fv and Fab format engineered with variable domains of different stability.* J Mol Biol, 2005. **347**(4): p. 773–89.

25. Asial, I., et al., *Engineering protein thermostability using a generic activity-independent biophysical screen inside the cell.* Nat Commun, 2013. **4**: p. 2901.

26. Rakestraw, J.A., et al., *Secretion-and-capture cell-surface display for selection of target-binding proteins.* Protein Eng Des Sel, 2011. **24**(6): p. 525–30.

27. Wu, M. and A.K. Singh, *Single-cell protein analysis.* Curr Opin Biotechnol, 2012. **23**(1): p. 83–8.

28. Mehling, M. and S. Tay, *Microfluidic cell culture.* Current Opinion in Biotechnology, 2014. **25**(0): p. 95–102.

29. Ma, C., et al., *A clinical microchip for evaluation of single immune cells reveals high functional heterogeneity in phenotypically similar T cells.* Nat Med, 2011. **17**(6): p. 738–43.

30. Han, Q., et al., *Polyfunctional responses by human T cells result from sequential release of cytokines.* Proc Natl Acad Sci U S A, 2012. **109**(5): p. 1607–12.

31. Benatuil, L., et al., *An improved yeast transformation method for the generation of very large human antibody libraries.* Protein Eng Des Sel, 2010. **23**(4): p. 155–9.

32. Shusta, E.V., et al., *Directed evolution of a stable scaffold for T-cell receptor engineering.* Nat Biotechnol, 2000. **18**(7): p. 754–9.

33. Brodsky, F.M., et al., *Monoclonal antibodies for analysis of the HLA system.* Immunol Rev, 1979. **47**: p. 3–61.